Published in final edited form as:
Nat Neurosci. 2020 October 01; 23(10): 1229–1239. doi:10.1038/s41593-020-0679-6.

Astrocytes Contribute to Remote Memory Formation by Modulating Hippocampal-Cortical Communication During Learning

Adi Kol[1], **Adar Adamsky**[1], **Maya Groysman**[2], **Tirzah Kreisel**[1], **Michael London**[1,3], **Inbal Goshen, Ph.D.**[1,§]

[1]Edmond and Lily Safra Center for Brain Sciences (ELSC), The Hebrew University of Jerusalem, Jerusalem, 91904 Israel

[2]ELSC Vector Core Facility, The Hebrew University of Jerusalem, Jerusalem, 91904 Israel

[3]Alexander Silberman Institute of Life Sciences, The Hebrew University of Jerusalem, Jerusalem, 91904 Israel

Abstract

Remote memories depend on coordinated activity in the hippocampus and frontal cortices, but the timeline of these interactions is debated. Astrocytes sense and modify neuronal activity, but their role in remote memory was scarcely explored. We expressed the Gi-coupled receptor hM4Di in CA1 astrocytes, and discovered that astrocytic manipulation during learning specifically impaired remote, but not recent, memory recall, and decreased activity in the anterior cingulate cortex (ACC) during retrieval. We revealed massive recruitment of ACC-projecting CA1 neurons during memory acquisition, accompanied by activation of ACC neurons. Astrocytic Gi activation disrupted CA3 to CA1 communication in-vivo, and reduced the downstream response in ACC. In behaving mice, it induced a projection-specific inhibition of CA1-to-ACC neurons during learning, consequently preventing ACC recruitment. Finally, direct inhibition of CA1-to-ACC projecting neurons spared recent and impaired remote memory. Our findings suggest that remote memory acquisition involves projection-specific functions of astrocytes in regulating CA1-to-ACC neuronal communication.

[§]To whom correspondence should be addressed: Inbal Goshen, Ph.D., Edmond and Lily Safra Center for Brain Sciences (ELSC), Givat Ram, Jerusalem 91904, The Hebrew University, Phone: 972-2-6585716, inbal.goshen@elsc.huji.ac.il.

Author Contribution

A.K. performed all in-vivo electrophysiology and 2-photon Calcium imaging experiments; A.A. contributed to behavioral experiments. MG produced AAV vectors. T.K. contributed to behavioral experiments and performed all projection targeting and histology. M.L. co-supervised electrophysiology experiments. I.G. conceived and supervised all aspects of the project, and wrote the manuscript with input from all other authors.

Competing Interests

The authors declare no competing interests

Accession Codes

N/A

Europe PMC Funders Author Manuscripts

Keywords

Astrocytes; Hippocampus; Anterior Cingulate Cortex (ACC); Fear conditioning; Remote Memory; Non Associative Place Recognition; In-Vivo Recording; 2-photon Calcium imaging; Chemogenetics; hM4Di; Optogenetics; cFos; Neurogenesis

Introduction

Remote memories, weeks to decades long, continuously guide our behavior, and are critically important to any organism, as the longevity of a memory is tightly connected to its significance. The ongoing interaction between the hippocampus and frontal cortical regions has been repeatedly shown to transform during the transition from recent (days long) to remote memory[1, 2, 3]. However, the exact time at which each region is recruited, the duration for which it remains relevant to memory function, and the interactions between these regions, are still debated.

Astrocytes are no longer considered to merely provide homeostatic support to neurons and encapsulate synapses, as pioneering research has shown they can sense and modify synaptic activity as an integral part of the 'tripartite synapse'[4]. Interestingly, astrocytes exhibit extraordinary specificity in their effects on neuronal circuits[5], at several levels: First, astrocytes differentially affect neurons based on their genetic identity. For example, astrocytes in the striatum selectively respond to, and modulate, the input onto two populations of medium spiny neurons, expressing either D1 or D2 dopamine receptors[6]. Similarly, astrocytes differentially modulate the effects of specific inhibitory cell-types but not others in the same brain region[7, 8, 9, 10], and selectively affect different inputs to the hippocampus[11]. Second, astrocytes exert neurotransmitter-specific effects on neuronal circuits. For instance, astrocytic activation in the central amygdala specifically depresses excitatory inputs and enhances inhibitory inputs[12]. Finally, astrocytes exhibit task-specific effects in-vivo, i.e. astrocytic stimulation selectively increases neuronal activity when coupled with memory acquisition, but not in the absence of learning[13]. An intriguing open question is whether astrocytes can also differentially affect neurons based on their distant projection target.

The integration of novel chemogenetic and optogenetic tools in astrocyte research allows real-time reversible manipulation of these cells at the population level, combined with electrophysiological and behavioral measurements. Such tools were used in brain slices to activate intracellular pathways in astrocytes, and show their ability to selectively modulate the activity of neighboring neurons in the amygdala and striatum[12, 14], and induce de-novo long-term potentiation in the hippocampus[13, 15]. Importantly, the reversibility of chemogenetic and optogenetic tools allows careful dissection of the effect of astrocytes during different memory stages in behaving animals[16, 17]. The recruitment of intracellular signaling pathways in astrocytes using such tools is starting to shed light on their complex involvement in memory processes, with Gq activation in the CA1 during acquisition (but not during recall) resulting in enhanced recent memory[13, 15], and Gs activation resulting in recent memory impairment[18].These findings point to the importance of astrocytes to memory processes, specifically at the time of learning.

To explore the role astrocytes in memory acquisition, we used the hM4Di receptor to activate the Gi pathway in these cells, and found that this astrocytic modulation in CA1 during learning resulted in a specific impairment in remote (but not recent) memory recall, accompanied by decreased activity in the anterior cingulate cortex (ACC) at the time of retrieval. In-vivo Gi activation in astrocytes disrupted synaptic transmission from CA3 to CA1, and reduced the downstream recruitment of the ACC. Finally, we reveal a dramatic recruitment of CA1 neurons projecting to ACC during memory acquisition, and a projection-specific inhibition of this population by Gi pathway activation in CA1 astrocytes. Indeed, when we directly inhibited only CA1-to-ACC projecting neurons, recent retrieval remained intact, whereas remote memory was impaired.

Results

Gi pathway activation in CA1 astrocytes specifically impairs the acquisition of remote memory

To specifically modulate the activity of the Gi pathway in CA1 astrocytes we employed an AAV8 vector encoding the designer receptor hM4Di fused to mCherry under the control of the astrocytic GFAP promoter. Stereotactic delivery of this AAV8-GFAP::hM4Di-mCherry vector resulted in CA1-specific expression, restricted to astrocytic outer membranes (Fig.1A,B), with high penetrance (>85% of GFAP cells expressed hM4Di), and the promoter provided almost complete specificity (>95% hM4Di+ cells were also GFAP+)(Extended Data Fig.1A-B). Co-staining with the neuronal marker NeuN showed less than 1% overlap with hM4Di expression (Extended Data Fig.1C,D).

Recent work has shown that hM4Di activation in astrocytes mimics the response of these cells to GABAergic stimuli[14, 19], and induces elevated expression of the immediate-early gene cFos in-vivo[14, 19, 20]. To verify this effect in our hands, mice were injected with CNO (10mg/kg, i.p.), brains were collected 90 min later and stained for cFos. As expected, CNO dramatically increased cFos levels in astrocytes of hM4Di-expressing mice, compared to Saline-injected controls ($t_{(9)}$=16.7; p=2.2E^{-8})(Fig.1C). As cFos is similarly induced by the recruitment of the Gq pathway[13, 20], it seems to be an unreliable indicator of the nature of astrocytic activity, signaling only the occurrence of a significant modulation. Thus, to better characterize the effect of Gi pathway activation in astrocytes at a time frame more relevant to behavioral experiments (executed tens of minutes after CNO administration), we performed prolonged 2-photon imaging in brain slices, using Ca^{2+} levels as a proxy for astrocytic activity. CA1 astrocytes expressing both hM4Di and GCaMP6f were imaged before and after application of ACSF or CNO (10μM)(Fig.1D-E,Extended Data Fig.1E-H). CNO triggered a mild decrease in baseline intracellular Ca^{2+} levels in hM4Di-expressing astrocytes ($t_{(395)}$=1.8; p=0.033)(Fig.1F), and reduced the total size of Ca^{2+} events in these cells ($t_{(400)}$=3.5; p=0.0005)(Fig.1G), compared to astrocytes treated with ACSF. We have shown in the past that CNO alone without DREADDs expression has no effect on calcium activity in astrocytes in the same timeframe[13]. Thus, we find that the reported initial increase in calcium activity in astrocytes following Gi pathway activation recruitment[14, 19], which is sufficient to induce cFos expression in-vivo (Fig.1C), is accompanied later by a decrease in

calcium dynamics, as opposed to Gq-mediated astrocytic activation, which results in both acute and minutes-long increases in calcium activity[13].

Previous elegant research demonstrated the necessity of normal astrocytic metabolic support to memory, and showed that chronic genetic manipulations in astrocytes affect memory acquisition and maintenance[21]. The contribution of astrocytes to remote memory acquisition, however, was never investigated. To address this topic, we took advantage of the temporal flexibility offered by chemogenetic tools, allowing not only cell type-specific, but also memory-stage specific (e.g. during acquisition or recall), reversible modulation of astrocytes, as we have recently used to show that activation of the Gq pathway in astrocytes enhances recent memory acquisition, but has no effect at the time of memory recall[13].

To test the effect of astrocytic Gi pathway modulation on cognitive performance, mice were injected bilaterally with AAV8-GFAP::hM4Di-mCherry into the dorsal CA1, and three weeks later CNO (10mg/kg, i.p.) was administered 30 minutes before fear conditioning (FC) training, pairing a foot-shock with a novel context and an auditory cue. CNO application in GFAP::hM4Di mice had no effect on context exploration (Extended Data Fig.2A) or on baseline freezing (Fig.1H *left*) before shock administration. One day later, when CNO was no longer present, mice were placed back in the conditioning context and freezing was quantified. We found no difference in recent memory retrieval between GFAP::hM4Di mice treated with CNO or Saline during FC acquisition (Fig.1H *right*). Remarkably, when the same mice were tested in the same context 20 days later, those treated with CNO during conditioning showed a dramatic impairment in memory retrieval ($t_{(10)}$=2.2; p=0.028)(Fig.1I *left*). This deficiency was still clearly observed 45 days after that, when mice were re-tested in the same context for a third time ($t_{(11)}$=3.5; p=0.0025)(Fig.1I *right*). The effect of CA1 astrocytic manipulation was unique to the hippocampal-dependent contextual memory task, as no effect was observed when the same mice were tested for auditory-cued memory in a novel context, i.e. both groups demonstrated similar freezing in response to the tone one day after training ($F_{(1,11)}$=94.2, time main effect, p=9.97E^{-7}), and 20 days later ($F_{(1,11)}$=13.4, time main effect, p=0.004)(Extended Data Fig.2B-C).

To verify that the observed effects are not the result of minor off-target hM4Di expression in neurons, we then tested what effects would inhibition of CA1 neurons have on recent and remote memory recall. We injected mice with an AAV5-CaMKIIα::hM4Di-mCherry vector to induce hM4Di expression in ~20% of CA1 glutamatergic neurons (Extended Data Fig. 2D). To test the effect of direct neuronal inhibition on recent and remote memory acquisition, we injected CaMKIIα::hM4Di mice with CNO (10mg/kg, i.p.) 30 minutes before FC acquisition. Gi pathway activation in neurons had no effect on the exploration of the conditioning cage before tone and shock administration (Extended Data Fig.2E), or on baseline freezing levels (Fig.1J *left*). Mice were then fear-conditioned, and tested on the next day. As expected, neuronal inhibition during training resulted in impaired contextual freezing one day later ($t_{(17)}$=3; p=0.004)(Fig.1J *middle*). When the same mice were tested in the same context 20 days later, the memory impairment was still apparent ($t_{(17)}$=1.8; p=0.046)(Fig. 1J *right*). No significant effect on auditory-cued memory in a novel context was observed, at either the recent or the remote time points, as both groups demonstrated similar freezing in response to the tone (time main effect $F_{(1,17)}$=155.4, p=5.59E^{-10} and

$F_{(1,17)}$=34.7, p=1.77E^{-5}, respectively)(Extended Data Fig. 2F,G). Thus, neuronal inhibition during acquisition impairs both recent and remote memory.

Effects specific to remote, but not recent, memory were reported in the past in response to neuronal manipulations at the time of recall (e.g. [22, 23, 24]). Thus, we next tested the necessity of intact astrocytic function during the retrieval of recent and remote memory. CNO administration during recent and remote recall tests of contextual or auditory-cued memory had no effect on freezing levels compared to Saline-injected controls (Extended Data Fig.2H-J). This finding is similar to our previously reported lack of effect of Gq pathway manipulation during memory recall[13]. Thus, normal astrocytic activity is not required during either recent or remote recall, but only during memory acquisition.

To further validate the unexpected effect of astrocytic Gi pathway activation during acquisition on remote memory in a less stressful task, we employed the 'non-associative place recognition' (NAPR) paradigm. In this task, mice explore a novel open field, and upon re-exposure to the same arena are expected to display decreased exploration of this now familiar environment. Indeed, GFAP::hM4Di mice injected with either Saline or CNO during NAPR acquisition showed a marked decrease in exploration upon a second exposure to the square environment to which they were exposed 1 day earlier, as expected ($F_{(1,12)}$=45.7, no interaction, time main effect p =2.01E^{-5})(Fig.1K). In a new cohort of GFAP::hM4Di mice,exploration upon the second exposure to a round environment which they originally explored 4 weeks earlier, was markedly reduced in mice injected with Saline during NAPR acquisition, as expected. However, exploration level in CNO-treated GFAP::hM4Di mice did not decrease (Fig.1L *left*), suggesting that they did not recall their remote experience in this context. These findings were reflected in a significant treatment by time interaction ($F_{(1,11)}$=15.98, p=0.002), and post-hoc analysis showed a significant difference between the first and second visit only for the Saline group (p=0.001). A significant effect was also found for the decrease in exploration between Saline and CNO treated mice ($t_{(11)}$=-2.8; p=0.0085)(Fig.1L *right*). To confirm that these mice are still capable of performing NAPR normally when astrocytic activity is intact, and verify the absence of non-specific long-term effects, we repeated the experiment in a novel trapezoid environment with no CNO administration in the same cohort, which now demonstrated comparable performance between groups ($F_{(1,11)}$=14.89, time main effect p=0.003, no interaction)(Extended Data Fig.2K).

To verify that our results did not stem from the CNO application itself, control mice injected with an AAV8-GFAP::eGFP vector were trained in the same behavioral paradigms. CNO administration (10mg/kg, i.p.) in these mice had no effect on baseline freezing, recent or remote contextual memory, or on performance in the remote NAPR task ($F_{(1,11)}$=58.7, time main effect p=9.86E^{-6}, no interaction)(Extended Data Fig.3A-D).

Our results show that Gi activation in CA1 astrocytes during the acquisition of spatial memory selectively impairs its remote, but not recent, recall, whereas direct neuronal inhibition during acquisition impairs both recent and remote memory. These findings raise two novel hypotheses: First, that the foundation for remote memory is established during acquisition in a parallel separate process to recent memory, and can thus be manipulated

independently. Second, that astrocytes are able to specifically modulate the acquisition of remote memory, with precision not granted by general neuronal inhibition. Both hypotheses are tested below.

Astrocytic Gi pathway activation during memory acquisition reduces the recruitment of brain regions involved in remote memory, during retrieval

The transition from recent to remote memory is accompanied by brain-wide reorganization, including the recruitment of frontal cortical regions like the ACC[1, 2, 3, 23, 25, 26, 27], indicated by increased expression of cFos[23,25]. To gain insight into changes in the neuronal activity accompanying the recent and remote retrieval of memories acquired under astrocytic modulation, GFAP::hM4Di mice were injected with Saline or CNO before FC acquisition, brains were collected 90 minutes after recent or remote recall, stained for cFos, and quantified in neurons at CA1 and ACC (Fig.2A), areas repeatedly implicated in remote memory[2, 28]. As before, CNO administration toGFAP::hM4Di mice during acquisition had no effect on recent contextual memory (Fig.2B), and no changes in cFos expression following recent recall in either CA1 or ACC were observed (Fig.2C-E). Another cohort of GFAP::hM4Di mice was injected with CNO before acquisition, tested for recent memory 24 hours later, and then for remote recall 21 days after that. Importantly, we replicated our initial finding that astrocytic modulation during acquisition specifically impaired remote but not recent contextual memory ($t_{(9)}$=2.6; p=0.014)(Fig.2F). Impaired remote memory was accompanied by reduced cFos expression in both the CA1 ($t_{(7)}$=2.6; p=0.0175) and the ACC ($t_{(7)}$=2.61; p=0.0175) regions (Fig.2G-I). We also performed the same cFos quantification in brains collected after the last recall test from the first behavioral experiment (Fig.1I), of mice that were injected with CNO >60 days earlier. In this experiment too, impaired remote recall in GFAP::hM4Di mice treated with CNO during conditioning was accompanied by reduced cFos expression in CA1 and ACC compared to Saline treated mice ($t_{(12)}$=2.01, p=0.029; $t_{(7)}$=1.97; p=0.04)(Extended Data Fig.4B).

In the same mice we also quantified retrieval-induced cFos expression in several additional brain regions known to be involved in memory: The Dentate Gyrus (DG) of the hippocampus, the Retrosplenial Cortex (RSC), and the Basolateral Amygdala (BLA). No changes in cFos expression in the DG or RSC were observed. BLA cFos expression was reduced in GFAP::hM4Di mice treated with CNO ($t_{(6)}$=3; p=0.01p=0.011)(Extended Data Fig.4A,C). Finally, to exclude any non-specific effects of CNO itself, we repeated the same experiments in control GFAP::eGFP mice. As before, CNO application alone induced no difference in either recent or remote fear memory, and we found no alterations in cFos expression (Extended Data Fig.4D-K).

Again, we show that astrocytic Gi pathway activation during fear memory acquisition selectively impaired remote recall, but spared recent retrieval. Moreover, this memory deficiency was accompanied by reduced activity not only in the CA1, where astrocytes were modulated, but also in the ACC, three weeks after manipulation. This temporal association, however, does not necessarily indicate causality, and two possible explanations can be offered: 1) that astrocytic Gi activation induces a long-term process whose consequences are

only observed weeks later, or 2) that it acutely impairs the acquisition of remote (but not recent) memory. We test both options below.

Modulation of CA1 astrocytes has no effect on hippocampal neurogenesis

Our findings of intact recent memory followed by impaired remote memory and reduced hippocampal activity could suggest that astrocytic modulation during acquisition initiated a long-term process that took weeks to convey its effect. One example for such a process could be hippocampal neurogenesis occurring between recent and remote recall, which had been repeatedly shown to reduce remote memory[29], thus we sought to examine whether astrocytic manipulation induced changes in neurogenesis. To tag newborn cells, we administered BrdU (100mg/kg, i.p.) together with the CNO or Saline injection to GFAP::hM4Di mice, 30min before acquisition, and another dose 2hr after training. Brains from mice tested for recent retrieval were stained for BrdU, tagging the cells added to the DG since the previous day[30]. No changes in proliferation or in the number of cells expressing Doublecortine (DCx), a marker of young neurons 3 days to 3 weeks old, were observed (Fig.2J-L). Similarly, in brains collected after remote recall no changes in the survival of cells formed on the day of acquisition three weeks previously, or their differentiation fate (determined by co-staining with the neuronal marker NeuN) were observed. Additionally, no change in the number of young neurons born during these three weeks, marked by DCx, was observed (Fig.2M-O).CNO application in GFAP::eGFPcontrol mice had no effect on neurogenesis 24 hours or 21 days later (Extended Data Fig.4L-Q).

To conclude, astrocytic manipulation in CA1 had no effect on hippocampal neurogenesis, and thus an alternative mechanism to the selective impairment of remote memory was subsequently investigated.

Gi pathway activation in CA1 astrocytes prevents the recruitment of the ACC during memory acquisition

Our findings show that remote memory performance and cFos levels in CA1 and ACC are temporally associated, i.e. when remote recall is low so are cFos levels at the time of recall, but it is challenging to conclude which phenomenon underlies the other. Furthermore, the temporal distance between the appearance of these phenotypes and the astrocytic manipulation three weeks earlier makes it hard to determine exactly when they were induced. We thus tested the immediate effects of CA1 astrocytic modulation on neuronal activity during memory acquisition. GFAP::hM4Di mice were injected with Saline or CNO before FC acquisition, and brains were collected 90 minutes later (Fig.3A). CNO administration had no effect on foot-shock-induced immediate freezing (Extended Data Fig.5A). To control for the effect of astrocytic manipulation on neuronal activity, independent of learning, we manipulated astrocytes in home-caged mice. cFos expression was quantified in the CA1, ACC, BLA, DG and RSC. Fear conditioning acquisition induced an overall increase in cFosexpression in the CA1, ACC and BLA ($F_{(1,21)}$=8.1, p=0.01; $F_{(1,17)}$=5.07, p=0.038; $F_{(1,16)}$=9.07, p=0.008; respectively), but not in the DG and RSC (Fig.3B-D; Extended Data Fig.5B-H). Astrocytic manipulation in CA1 did not significantly affect local neuronal cFos expression in this region in either home-caged or fear-conditioned mice (Fig.3B-C;Extended Data Fig.5C). To verify that the increase in ACC cFos following

acquisition does not represent astrocytic activation in this region, we co-stained for cFos and GFAP, and found only a negligible amount of cFos-expressing astrocytes (Extended Data Fig.5I).

Surprisingly, Gi activation in CA1 astrocytes significantly reduced the learning-induced elevation in cFos expression in the ACC, where no direct manipulation took place (Fig.3B,D; Extended Data Fig.5D). This result is reflected by a significant treatment by behavior interaction ($F_{(1,17)}$=5.04, p<0.05; FC-Saline vs. FC-CNO post-hoc, p<0.05). The effect was specific to the ACC, and not observed in other non-manipulated regions, like the BLA, DG or RSC (Extended Data Fig.5E-H).

The finding that astrocytic Gi pathway activation in CA1 prevented the recruitment of the ACC during learning suggests a functional CA1→ACC connection, which can be modulated by hippocampal astrocytes. The existence of a monosynaptic CA1→ACC projection had been demonstrated[31], and a functional connection was reported using electrical stimulation[32]. To generate synaptic input to CA1 we expressed channelrhodopsin-2 (ChR2) in CA3 (Fig.3E,F), a major CA1 input source. ChR2-expressing axons from CA3 were observed in the CA1 stratum radiatum, and hM4Di was concomitantly expressed in CA1 astrocytes (Fig.3E,G). Importantly, no fluorescence was detected in the ACC, as there is no direct CA3→ACC projection (Extended Data Fig.5J,K). Light was applied to CA1 in anesthetized mice, via a fiber coupled to an electrode recording the neuronal response in CA1 (Fig.3H). A second electrode was placed in the ACC to record the downstream response to CA1 activation (Fig.3H, Extended Data Fig.5J,K). Recordings were performed after i.p. Saline administration and then after i.p. CNO administration. Optogenetic stimulation of the Schaffer collaterals induced a local response in CA1, which was mildly but significantly reduced by CNO injection (paired $t_{(3)}$=2.6; p=0.04)(Fig. 3I,J). Astrocytic manipulation in the CA1 had a dramatic effect on the downstream response in the ACC to stimulation of the Schaffer collaterals, reflected by a significantly attenuated fEPSPs following CNO administration (paired $t_{(4)}$=3.8; p=0.01)(Fig.3K,L). These results suggest that astrocytic manipulation in CA1 can indeed modulate the functional connectivity from CA1 to ACC.

We show that Gi pathway activation in CA1 astrocytes during fear memory acquisition prevented the recruitment of the ACC, without having a significant effect on local neuronal activity in the CA1, and that CA1 astrocytes can indeed modulate the functional CA1→ACC connectivity. These findings suggest that astrocytic manipulation selectively blocked the activity of CA1 neurons projecting to the ACC, resulting in a significant effect on ACC activity, but only a mild influence on total CA1 activity.

Gi activation in CA1 astrocytes during memory acquisition specifically prevents the recruitment of CA1 neurons projecting to ACC

From our findings that Gi activation in CA1 astrocytes during learning prevented the recruitment of the ACC, and that CA1 astrocytes are able to modulate CA1→ACC functional connectivity, we drew the hypothesis that astrocytic Gi activation can selectively prevent the recruitment of CA1 neurons projecting to the ACC, without similarly affecting other CA1 neurons.

To directly test this hypothesis, we tagged these projection neurons, measured their recruitment during memory acquisition, and how it is affected by astrocytic Gi activation. Mice were bilaterally injected with a retro-AAV inducing the expression of the Cre recombinase in excitatory neurons (AAV-retro-CaMKIIα::Cre) into the ACC, and an additional Cre-dependent virus inducing the expression of GFP (AAV5-ef1 α::DIO-GFP) into CA1.AAV8-GFAP::hM4Di-mCherry was simultaneously injected into the CA1, to allow astrocytic manipulation (Fig.4A). Together, these three vectors induced the expression of GFP only in CA1 neurons projecting to the ACC, and of hM4Di in hippocampal astrocytes (Fig.4B-C).These mice were injected with Saline or CNO 30 minutes before FC acquisition or in their home cage, and brains were collected 90 minutes later. As in the previous experiment, CNO administration had no effect on immediate freezing following shock administration, FC acquisition induced an overall increase in cFos expression in the CA1 ($F_{(1,21)}$=12.9 p=0.002), and astrocytic modulation was not sufficient to significantly reduce CA1 cFos expression (Fig.4D-E). Furthermore, as before, modulation of CA1 astrocytes significantly reduced the learning-induced elevation in ACC cFos expression ($t_{(13)}$=1.78, p=0.049)(Fig.4E).

When specifically observing the sub-population of CA1 neurons projecting to ACC, these cells were found to be dramatically recruited during memory acquisition, and astrocytic modulation significantly reduced the learning-induced cFos elevation in this population (Fig.4F). Specifically, in Saline treated mice, more than 15% of CA1→ACC cells expressed cFos following learning, whereas in CNO-treated GFAP::hM4Di mice less than 5% CA1→ACC cells were active after learning, a level as low as that of home-caged mice (Fig.4F-H; Extended Data Fig.6A,B). This effect resulted in a significant treatment by behavior interaction ($F_{(1,21)}$=6.67, p=0.017; FC-Saline vs. FC-CNO post-hoc p=0.001).

Finally, to test the specificity of our findings, we similarly tested an additional monosynaptic projection from the CA1, terminating at the Nucleus Accumbens (NAc). Mice were bilaterally injected with AAV-retro-CaMKII::Cre into the NAc, together with AAV5-ef1α::DIO-GFP and AAV8-GFAP::hM4Di-mCherry into CA1, to tag CA1 neurons projecting to the NAc, and activate the Gi pathway in CA1 astrocytes (Fig.4I-K). As in the previous experiment, CNO administration before FC acquisition had no effect on immediate freezing (Fig.4L-M). Activity in the NAc increased following fear conditioning ($F_{(1,22)}$=4.37 p=0.048), but importantly, modulation of CA1 astrocytes had no effect on cFos expression after learning in this region (Fig.4M; Extended Data Fig.6D,F). When we specifically tested cFos expression in the sub-population of NAc-projecting CA1 neurons, we found that these neurons are only mildly recruited by learning ($F_{(1,23)}$=4.41 p<0.047), and that astrocytic modulation had no effect on their activity (Fig.4N; Extended Data Fig.6C,E).

To conclude, we found that Gi pathway activation in CA1 astrocytes specifically prevented the exceptional recruitment of CA1→ACC projecting neurons during memory acquisition. The fact that the inhibition of this projection is induced by the same manipulation that specifically impairs remote memory acquisition, suggests that the activity of CA1→ACC neurons during memory acquisition is necessary for remote recall.

Specific inhibition of CA1 neurons projecting to ACC impairs the acquisition of remote, but not recent, memory

To specifically manipulate CA1→ACC neurons, mice were bilaterally injected with AAV-retro-CaMKIIα::Cre into ACC, and a Cre-dependent hM4Di virus (AAV5-ef1α::DIO-hM4Di-mCherry) into CA1 (Fig.5A). Together, these vectors induced the expression of hM4Di-mCherry only in CA1 neurons projecting to the ACC (Fig.5B-C). Three weeks later, mice were injected with Saline or CNO 30 minutes before FC acquisition. CNO application in CA1→ACC-hM4Di mice had no effect on the exploration of the conditioning cage before shock administration(Extended Data Fig.7A), on baseline freezing before shock delivery, or on recent memory (Fig.5D *left&middle*). However, when the same mice were tested in the same context 20 days later, those treated with CNO during conditioning demonstrated impaired remote retrieval (t(16)=1.8;p=0.048)(Fig.5D *right*). The effect of specific CA1→ACC neurons inhibition was unique to the hippocampal-dependent contextual memory task, as no effect was observed when the same mice were tested for auditory-cued memory in a novel context, i.e. both groups demonstrated similar freezing in response to the tone one day after training and 20 days later ($F_{(1,16)}$=147.8, p=1.7E^{-9}; $F_{(1,16)}$=37.8, p=1.4E^{-5},time main effect, respectively)(Extended Data Fig.7B-C).

Finally, to gain insight into changes in the neuronal activity accompanying this impaired remote retrieval of memories acquired underCA1→ACC projection inhibition, brains were collected 90 minutes after remote recall, and stained forcFos. We found that the impaired remote memory was accompanied by reduced cFos expression in both the CA1 ($t_{(15)}$=-2.2,p=0.022) and the ACC ($t_{(14)}$=-2.4,p=0.015) regions (Fig.5E,G,H). When specifically observing theCA1→ACC neurons manipulated three weeks earlier, we found significantly reduced cFosexpression ($t_{(14)}$=-2,p=0.033)(Fig.5F,G).

In this experiment, we directly prove the involvement of CA1→ACC neurons in establishing the foundation for remote memory during acquisition, as suggested by the effect of astrocytes on this process.

Discussion

Recent years have seen a burst in discoveries of hitherto unknown elaborate roles for astrocytes in the modulation of neuronal activity and plasticity[21]. In this work, we show for the first time that these cells can confer specific effects on neurons in their vicinity based on the distant projection target of these neurons. Specifically, astrocytic Gi activation during memory acquisition impairs remote, but not recent, memory retrieval. Another novel finding we present is a massive recruitment of ACC- projecting CA1 neurons during memory acquisition, a process specifically inhibited byastrocytic manipulation, thus preventing a successful recruitment of the ACC during learning. Finally, we directly inhibit this projection to prove its necessity for the formation of remote memory.

Chemogenetic and optogenetic tools, originally developed for use in neurons and allowing real-time, reversible, cell-specific manipulation, are now integrated into astrocyte research.Chemogenetic tools recruit intracellular pathways in astrocytes, toinduce clear behavioral effects, which vary greatly depending on the modulated cellular

mechanism[12, 13, 14, 18, 33]. For example, in our hands Gq pathway activation in astrocytes (via Hm3Dq) leads to recent memory enhancement[13], whereas in this work we report that Gi pathway activation has no effect on recent memory, and specifically impairs remote memory. In contrast to these clear differences in the downstream physiological and behavioral effects of astrocytic manipulation, the intracellular calcium dynamics recorded in the astrocytes in reaction to very different stimuli are very much alike. For example, despite the fact that the Gq and Gi pathways are endogenously recruited by the administration of different neurotransmitters (e.g. Gq by ACh and Gi by GABA), cFos expression in astrocytes is similarly induced by activating eitherof these pathways[13, 14, 19, 20, and Fig. 1C above], making it a good indicator for the occurrence of a modulation, but not to its precise nature. Similarly, chemogenetic activation of either the Gq or the Gi pathways induced an increase in intracellular calcium in astrocytes[13, 14, 19, 20]. However, whereas Gq pathway activation results in a long-lasting increase of Ca^{2+} activity[13], we found that the effect of Gi pathway activation wanes in time, and on a behaviorally-relevant timescale even decreases slightly. The discrepancy between the clear downstream functional differences of astrocytic modulation by Gq and Gi DREADDs, and the similarity in Calcium responses to these stimuli may be resolved in the future by advanced imaging and analysis methods providing insight to the intricacies of calcium signals in these cells[34].

Previous evidence suggests that astrocytes could have projection-specific effects, based on either the input source or the output target of their neighboring neurons, but with some caveats. For example, in the central amygdala, astrocytic activation depressed inputs from the basolateral amygdala, and enhanced inputs from the central-lateral amygdala[35]. However, since the former projection is excitatory, and the latter inhibitory, this finding could reflect specificity to the secreted neurotransmitter, rather than to the projection source. Additionally, astrocytes in the striatum specifically modulate either the direct or the indirect pathways[6]. Nonetheless, since the populations of striatal neurons from which these two projections originate differ genetically (expressing either the D1 or D2 dopamine receptors), it is impossible to determine whether the specificity astrocytes demonstrate stems from surface protein expression in these neurons or their projection target. Similarly, astrocytes in the DG may differentially affect input from the medial perforant path, but the terminals of this pathway differ from the lateral perforant path in their exclusive expression of the GluN3a NMDA subunit[11]. Here, we show for the first time differential effects of astrocytic modulation on CA1 pyramidal cells based exclusively on their projection target. These cells may differ from other CA1 cells in the configuration of inputthey receive, their activity pattern, and possibly even in hitherto unidentified genetic properties.

The leading hypothesis in the memory field was that the hippocampus has a time-limited role in memory – required for acquisition and recent recall, and becoming redundant for remote recall, being replaced by frontal cortices[2]. However, this temporal separation between the hippocampus and frontal cortex is not so rigid. For example, we and others have shown that the hippocampus is still critically involved in the consolidation and retrieval of remote memory (e.g.[23, 25, 36, 37, 38]). Current research now attempts to define the temporal dynamics in different brain regions underlying remote memory[25, 38]. The evidence regarding the role of frontal cortices during acquisition is mixed: Inhibition of medial entorhinal cortex input into PFC during acquisition specifically impaired remote

memory[39]. Conversely, inhibition of the PFC during acquisition had no effect on remote recall, nor did activation during remote recall of PFC neurons that were active during acquisition[40]. The role of the ACC in remote memory retrieval was repeatedly demonstrated by the finding that ACC inhibition during recall impairs remote but not recent memory in multiple tasks[e.g.22, 23, 24, 41, 42]. However, the time-point at which the ACC is recruited to support remote memories was never defined. Here, we show that the ACC is recruited at the time of initial acquisition, but the significance of this early activity is only revealed at the remote recall time point. We further demonstrate, for the first time, massive recruitment of ACC-projecting CA1 cells during learning, and show that specific inhibition of this projection at this time-point by astrocytes prevents the engagement of the ACC during acquisition, and results in impaired remote (but not recent) memory. When a non-specific CA1 inhibition is induced by direct neuronal Gi pathway activation, both recent and remote memory is impaired.

In this work, we reveal another novel capacity of astrocytes – to affect their neighboring neurons based on their projection target. This finding further expands the repertoire of sophisticated ways by which astrocytes shape neuronal networks and consequently high cognitive function.

Methods

Subjects

Male C57BL6 mice, 6-7 weeks old (Harlan) were group housed on a 12-hr light/dark cycle with *ad libitum* access to food and water. Experimental protocols were approved by the Hebrew University Animal Care and Use Committee and met guidelines of the National Institutes of Health guide for the Care and Use of Laboratory Animals. Mice were randomly assigned to experimental groups.

Virus Production

The pAAV-CaMKII-eGFP plasmid was made by first replacing the CMV promoter in a pAAV-CMV-eGFP vector with the CaMKII promoter. The pAAV-CaMKII-iCre plasmid was made by replacing the eGFP gene in the above plasmid with the coding region of iCre (Addgene 51904). Both pAAV-CaMKII-eGFP and pAAV-CaMKII-iCre plasmids were then packaged into AAV2-retro serotype viral vector. Similarly, pAAV-EF1-DIO-eGFP (Addgene 37084) plasmid was used to make the AAV5-EF1-DIO-eGFP viral vector. The above viral vectors were prepared at the ELSC Vector Core Facility (EVCF) at the Hebrew University of Jerusalem.

Viral vectors

AAV8-GFAP:: hM4D(Gi)-mCherry (UNC vector core, titer $7E^{12}$, diluted 1:10 in PBS when injected alone and 1:10 in other vector when injected with AAV5-EF1α::DIO-GFP, 700nl\site); AAV8-GFAP::eGFP (AAV8-GFAP::eGFP, titer $4.1E^{12}$, diluted 1:10 in PBS, 700 nl\site); AAV5-CaMKIIa::hChR2 (H134R)-eYFP (UNC vector core, titer $1.2E^{12}$, 250 nl\site); AAV5-EF1α::DIO-GFP (EVCF, titer $1.1E^{13}$, 500nl\site); AAV2-retro-CaMKII-

iCre (EVCF, titer $7E^{12}$, 400nl\site); AAV5-CaMKII::hM4Di-mCherry (EVCF, titer $1.1E^{13}$, 500nl\site);AAV5-GfABC1D::cytoGCaMP6F (Penn vector core, titer $6.13E^{13}$, 400nl/site).

Stereotactic Virus Injection

Mice were anesthetized with isoflurane, and their head placed in a stereotactic apparatus (Kopf Instruments, USA). The skull was exposed and a small craniotomy was performed. To cover the entire dorsal CA1, mice were bilaterally microinjected using the following coordinates: For CA1 (two sites per hemisphere), site 1:anteroposterior (AP), -1.5mm from bregma, mediolateral (ML), ± 1mm, dorsoventral (DV), -1.55mm; site 2: AP -2.5mm, ML ±2mm, DV -1.55mm. For ACC:AP 0.25mm, ML ± 0.4mm, DV -1.8mm. For Schaffer collaterals optogenetic activation, mice were bilaterally microinjected into the CA3 using the following coordinates: AP -1.85, ML +/-2.35, DV -2.25. All microinjections were carried out using a 10µl syringe and a 34 gauge metal needle (WPI, Sarasota, USA). The injection volume and flow rate (0.1µl/min) were controlled by an injection pump (WPI). Following each injection, the needle was left in place for 10 additional minutes to allow for diffusion of the viral vector away from the needle track, and was then slowly withdrawn. The incision was closed using Vetbond tissue adhesive. For postoperative care, mice were subcutaneously injected with Rimadyl (5mg per kg). See list of all vectors below.

Verification of hM4Di-mCherry expression spread

The expression area of hM4Di-mCherry was measured in all GFAP-hM4Di expressing mice. Mice with no expression were excluded from analysis. By figures, the average spread area (x1000pixels) was found to be: Figure 1D-E:191±46, Figure 2B-E: 178±18; Figure 3A-D:173±30; Figure 4A-H: 229±24. No significant differences were detected between the various experiments (one-way ANOVA, $F_{(3,72)}=2.63$; $p>0.05$).

Ca^{2+} Imaging in Hippocampal Slices

Coronal hippocampal slices (300µm) were made from 11-12 weeks old mice. Animals were anesthetized with isoflurane, and the brain was swiftly removed, mounted frontal-side up and sliced in ice-cold oxygenated low-calcium ACSF (see supplementary materials for the precise content of all solutions) using a vibratome (Campden Instruments). Slices were then incubated for 1hr in a holding chamber with oxygenated normal calcium ACSF at 35°C and then stored at 32°C. Individual slices were transferred to a submerged recording chamber (32°C), and astrocytes expressing both hM4D(Gi)-mCherry and GCaMP6f were selected for imaging.

Imaging was performed with a low-power temporal oversampling (LOTOS) two-photon microscope (LotosScan2015, Suzhou Institute of Biomedical Engineering and Technology http://english.sibet.cas.cn/). mCherry and GCaMP6f were excited at 920nm with a Ti:Sapphirelaser (Vision II, Coherent Inc., CA) and imaged through a 25X, 1.05 NA water immersion objective (Olympus, Japan).Red and green fluorescence signals were collected via two different PMTs. Full frame images (600 × 600 pixels) were acquired at 20 frames/second. Image acquisition was performed using a LabView based software (LotosScan), and images were analyzed with ImageJ (NIH) and Matlab.

Astrocytes were imaged 3 times for 3 minutes separated by 1 minute interval to determine baseline Ca^{2+} levels and activity. CNO or ACSF were then added to the chamber and imaging (3X3 minutes separated by 1 minute interval) was resumed after a ten minutes brake. Signal processing and analysis were conducted using ImageJ (NIH) and MatLab. Temporal series were imported into ImageJ, astrocytic somas and their main branches were identified by their GCaMP6f and mCherry co-expression, as well as their activity (measured by the standard deviation, and manually segmented as regions of interest (ROIs).

To determine the baseline intracellular calcium levels, we calculated the mode for each 3 minutes imaging epoch per ROI, then averaged the three epochs before and three epochs after the addition of CNO or ACSF. To quantify Ca^{2+} events, we computed the integral of theZ score for each three minutes imaging epoch from the florescence signal in each ROI. The Z score was calculated as $(F-\mu)/\sigma$, where μ and σ are the mean and standard deviation defined from the baseline histogram of F ($<90^{th}$ percentile). Negative Z scores were zeroed. We then averaged the z scores of the three epochs before and three epochs after the addition of CNO or ACSF. Epochs where the F signal throughout the 3 minutes had standard deviation lower than 1 were assigned a Z score of 0 for the entire epoch. ROIs where no active epochs were detected before and after manipulation were excluded from analysis.

Immunohistochemistry

3 weeks post-injection mice were transcardially perfused with cold PBS followed by 4% paraformaldehyde (PFA) in PBS. The brains were extracted, postfixed overnight in 4% PFA at 4°C, and cryoprotected in 30% sucrose in PBS. Brains were sectioned to a thickness of 40μm using a sliding freezing microtome (Leica SM 2010R) and preserved in a cryoprotectant solution (25% glycerol and 30% ethylene glycol, in PBS). Free-floating sections were washed in PBS, incubated for 1 h in blocking solution (1% bovine serum albumin (BSA) and 0.3% Triton X-100 in PBS), and incubated overnight at 4°C with primary antibodies (See full list of all antibodies below) in blocking solution. For the cFos staining, slices were incubated with the primary antibody for 5 nights at 4°C. Sections were then washed with PBS and incubated for 2 h at room temperature with secondary antibodies (See supplementary materials) in 1% BSA in PBS. Finally, sections were washed in PBS, incubated with DAPI (1μg/ml), and mounted on slides with mounting medium (Flouromount-G, eBioscience, San-Diego, CA, USA).

For neurogenesis staining, BrdU (Sigma 100mg/kg) was injected intraperitoneally together with the CNO injection, as well as 2 hours after the FC training. 90 minutes after recent or remote recall, brains were removed and slices prepared as described above. Sections were fixated in 50% formamide and 50% SSC for 2 hours in 65°C, then incubated in 2N HCl for 30min at 37°C and neutralized in boric acid for 10min. After PBS washes, sections were blocked in 1% BSA with 0.1% Triton-X for 1 hour at room temperature. Sections were incubated with anti-BrdU for 48h at 4°C. Sections were then washed with PBS and incubated with a secondary antibody for 2 hours at room temperature.

Antibodies

Primary antibodies—Chicken anti-GFAP (Millipore, Catalog # AB5541, diluted 1:500)[13], Rabbit anti-NeuN (Cell Signaling Technology, Catalog # 12943, diluted 1:400)[13], Rat anti-BrdU (Biorad, Catalog # OBT0030G, diluted 1:200)[30], Guinea pig anti-DCX (Millipore, Catalog # AB2253, diluted 1:1000)[30], Rabbit anti c-Fos (Synaptic Systems, Catalog # 226 003, diluted 1:10,000)[13]

Secondary antibodies—All from Jackson Laboratories. Donkey anti-chicken (conjugated to Alexa Fluor 488, Catalog # 703-545-155, diluted 1:500), Donkey anti-rabbit (conjugated to Alexa Fluor 488, Catalog # 711-545-152, diluted 1:500), Donkey anti-goat (conjugated to Alexa Fluor 594, Catalog # 705-585-147, diluted 1:400), Donkey anti-guinea pig (conjugated to Cy5, Catalog # 706-605-148, diluted 1:400) and Donkey anti-rat (conjugated to Cy5, Catalog # 712-175-153, diluted 1:400).

Confocal Microscopy

Confocal fluorescence images were acquired on an Olympus scanning laser microscope Fluoview FV1000 using 4X and 10X air objectives or 20X and 40X oil immersion objectives. Image analysis was performed using either ImageJ (NIH) or Fluoview Viewer version 4.2 (Olympus). Cells were counted blindly.

Behavioral Testing

The FC apparatus consisted of a conditioning box (18x18x30 cm), with a grid floor wired to a shock generator surrounded by an acoustic chamber (Ugo Basile), and controlled by the EthoVision software (Noldus). Three weeks after injections, mice were placed in the conditioning box for 2min, and then a pure tone (2.9 kHz) was sounded for 20sec, followed by a 2sec foot shock (0.4 mA). This procedure was then repeated, and 30sec after the delivery of the second shock mice were returned to their home cages. FC was assessed by a continuous measurement of freezing (complete immobility), the dominant behavioral fear response. Freezing was automatically measured throughout the testing trial by the EV tracking software. To test contextual FC, mice were placed in the original conditioning box, and freezing was measured for 5min. To test auditory-cued FC, mice were placed in a different context (a cylinder-shaped cage with stripes on the walls and a smooth floor), freezing was measured for 2.5min, and then a 2.9kHz tone was sounded for 2.5min, during which conditioned freezing was measured. Mice were tested for recent memory 24hr after acquisition, and for remote memory 21 or 28 days later. In one experiment, an additional remote memory test was performed 66 days after acquisition.

The non-associative place recognition (NAPR) test was conducted in around plastic arena, 54 cm in diameter or a square or a trapezoid arena with an identical area size (2290cm^2). Mice were placed in the center of the arena and allowed to freely explore for 5 min. Habituation to the familiar environment (reduced exploration between first and second exposures) was measured using the EthoVision tracking software.

CNO (Tocris) was dissolved in DMSO and then diluted in 0.9% saline solution to yield a final DMSO concentration of 0.5%. Saline solution for control injections also consisted

of 0.5% DMSO. 10mg/kg CNO was intraperitoneally (i.p.) injected 30min before the behavioral assays. In the relevant experiments, BrdU (sigma B5002, 100mg/kg) was injected i.p. together with the CNO/Saline and 2 hours after the behavioral experiment.

In-vivo Electrophysiology and Optogenetics

Simultaneous optical stimulation of the Schaffer Collaterals and electrical recordings in CA1 and ACC were performed as follows: Mice were anesthetized with isoflurane, and an optrode (an extracellular tungsten electrode (1MΩ, ~125μm) glued to an optical fiber (200μm core diameter, 0.39 NA) with the tip of the electrode protruding ~400μm beyond the fiber end) was used to record local field potential in Stratum Radiatum and illuminate the Schaffer Collaterals. fEPSP recordings were conducted with the optrode initially placed above the dorsal CA1 (AP -1.6mm; ML 1.1mm; DV -1.1mm) and gradually lowered in 0.1mm increments into the Stratum Radiatum (-1.55mm). The optical fiber was coupled to a 473nm solid-state laser diode (Laserglow Technologies, Toronto, Canada)with ~10mW of output from the fiber. fEPSPrecordings from the ACC were similarly performed using an extracellular tungsten electrode (1MΩ, ~125μm) placed over the ACC (AP 0.25mm; ML 0.4mm; DV -1.3mm) and gradually lowered in 0.1mm increments to 1.8DV. This electrode was dipped in DiI (1mg/1.5ml in 99% ethanol; Invitrogen) to validate the position of the recording site.

To optogenetically activate the Schaffer collaterals, blue light (473 nm) was unilaterally delivered through the optrode. Photostimulation duration was 10 ms, delivered 72 times for each treatment (Saline or CNO) every 5 seconds. Saline and CNO were injected i.p. and recording started 30 minutes after each injection.

Recordings were carried out using a Multiclamp 700B patch-clamp amplifier (Molecular Devices). Signals were low-pass filtered at 5 kHz, digitized and sampled through an AD converter (Molecular Devices) at 10 kHz, and stored for off-line analysis using Matlab (Mathworks Inc.). CA1 responses to Schaffer collaterals stimulation were quantified by calculating the amplitude of the fEPSPs relative to the mean baseline levels, defined as a 200ms time window prior to photostimulation. CA1 activation by Schaffer collaterals stimulation resulted in a complex downstream activity in ACC, lasting approximately 400ms. Because this signal had both positive and negative peaks, to estimate the overall magnitude of the response, we have calculated its mean absolute value over the entire 400ms period, from the beginning of photostimulation in CA1.

Statistical Analysis

The results of automatic or blind measurements were analyzed by a two-way ANOVA followed by LSD post-hoc tests, or by Student’s t test, both one-sided, as applicable. Data distribution was assumed to be normal but this was not formally tested. No statistical methods were used to pre-determine sample sizes but our sample sizes are similar to those reported in previous publications[13].

Europe PMC Funders Author Manuscripts

Extended Data

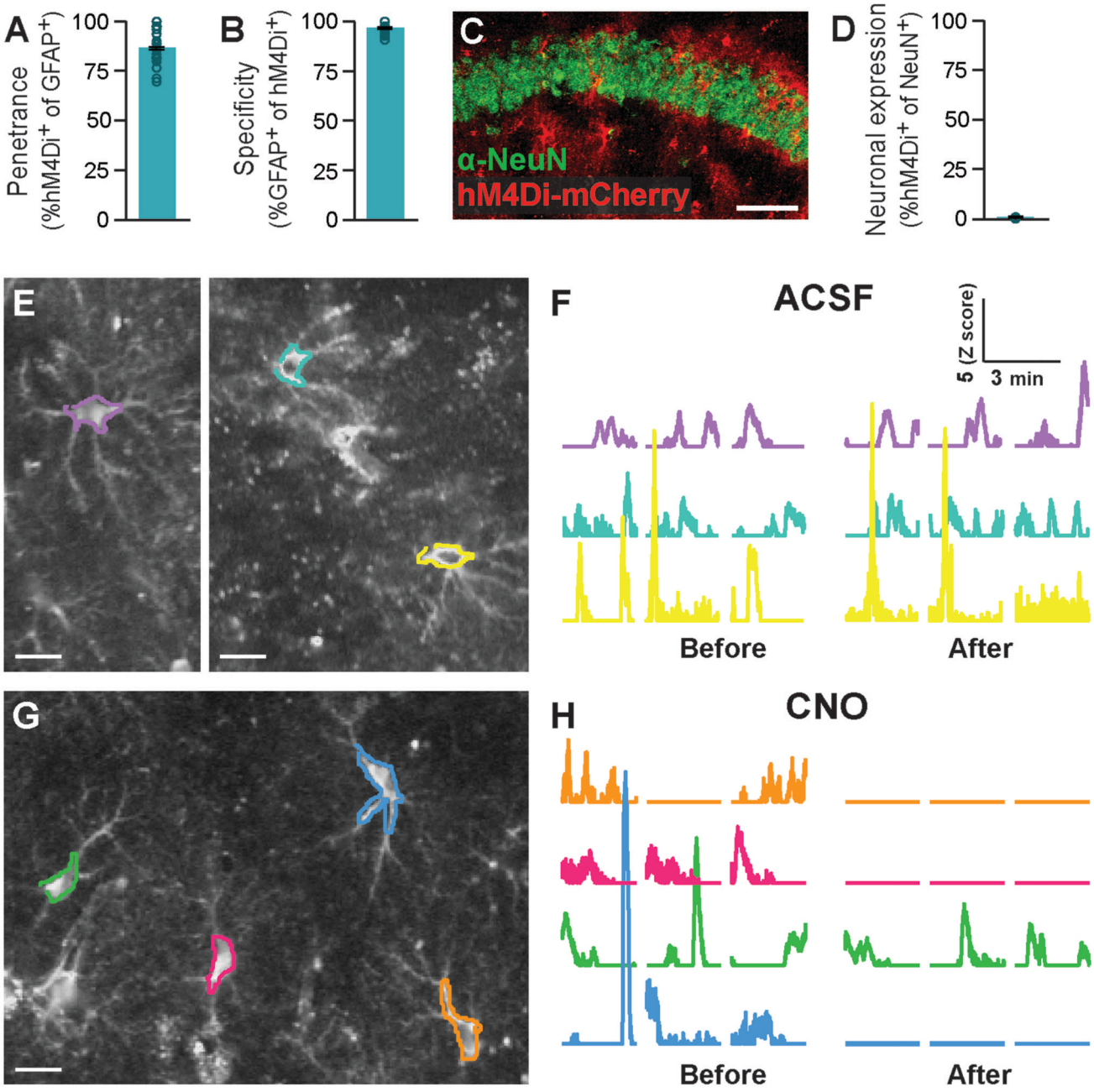

Extended Data Fig. 1. Prolonged Gi pathway activation in CA1 astrocytes reduces their calcium activity (Related to Figure 1).

Following an injection of AAV8-GFAP::hM4Di-mCherry, hM4Di was expressed in 87% (491/552 cells from 4 mice) of CA1 astrocytes (**A**), with >96% specificity (491/507 cells, from 4 mice)(**B**). (**C-D**) Minimal co-localization with the neuronal nuclear marker NeuN was detected (scale bar 50μm; 0.9% expression in neurons, 7/766 cells). (**E,G**) Representative astrocytes expressing GCaMP6f (white) and hM4Di-mCherry (not visible,

but see Figure 1D) were exposed either to ACSF (**E,F**) or CNO (**G,H**). Representative ROIs, and their activity in corresponding colors are presented. Scale bars = 100μm.CNO application triggered a decrease in baseline intracellular Ca^{2+} levels, and reduced the total size of Ca^{2+} events in these cells (see Figure 1F,G). Data presented as mean ± standard error of the mean (SEM).

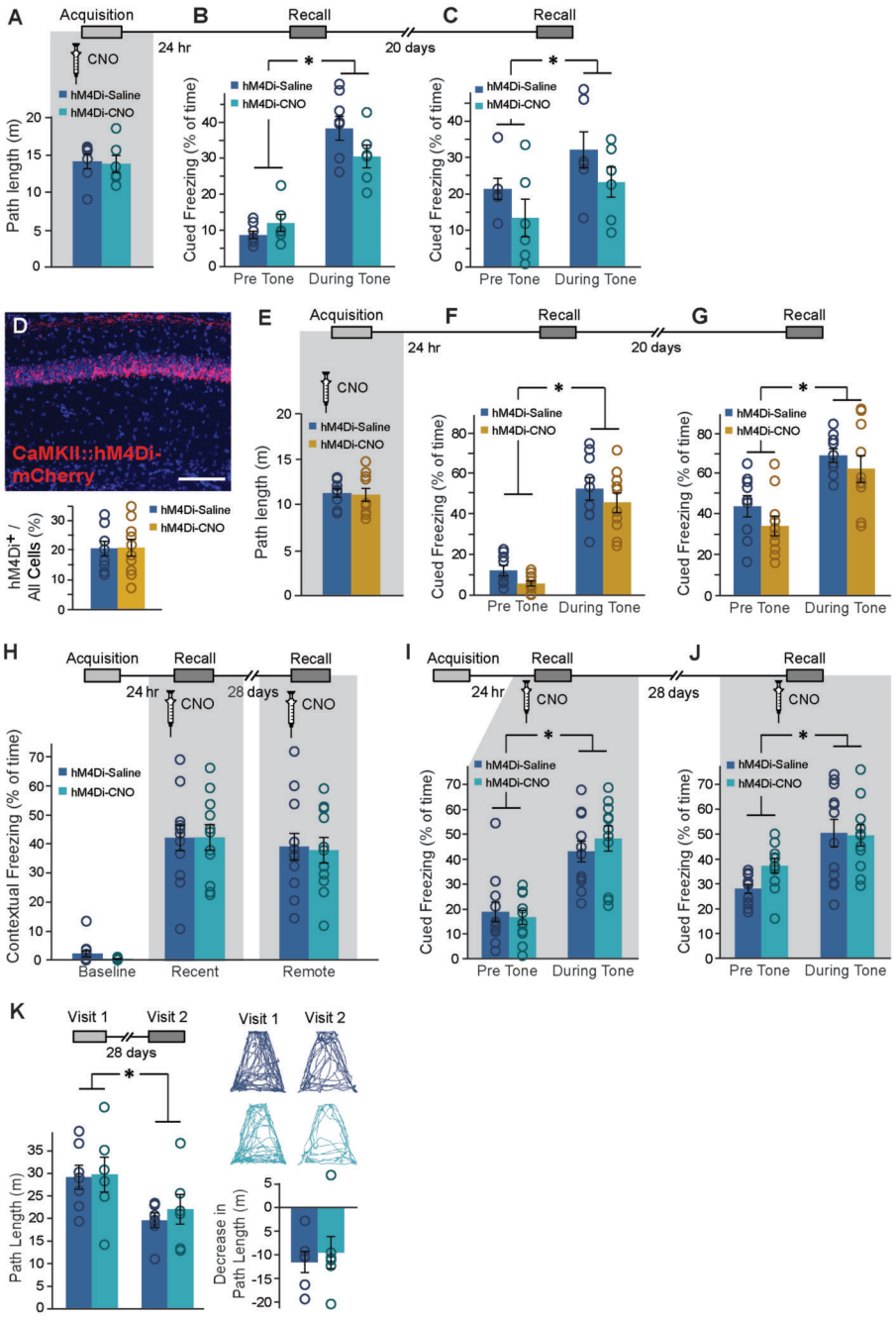

Extended Data Fig. 2. Astrocytic Gi activation in CA1 during learning had no effect on auditory-cued remote memory (Related to Figure 1).

GFAP::hM4Di mice were injected with Saline (n=7) or CNO (n=6) 30 min before Fear Conditioning (FC) acquisition. CNO application before training had no effect on exploration of the conditioning cage (**A**), or on auditory-cued memory recall either 24 hr after acquisition (**B**) or 20 days after that (**C**) in a novel context, with both groups showing increased freezing during tone presentation ($p<0.001$, $p<0.01$, respectively). (**D**) Bilateral double injection of AAV5-CaMKIIα::hM4Di-mCherry resulted in hM4Di-mCherry expression in CA1 Neurons only (*top*). Scale bar - 100 μm. The groups did not differ in the percent of hM4Di-expressing cells level of expression (Saline - 20.5%, CNO - 20.6%; *bottom*). CaMKIIα::hM4Di mice were injected with either Saline (n=9) or CNO (n=10) 30min before FC acquisition. CNO application before training had no effect on exploration of the conditioning cage (**E**), or on auditory-cued memory recall either 24 hr after acquisition (**F**) or 20 days after that (**G**) in a novel context, with both groups showing increased freezing during tone presentation ($p<0.000001$, $p<0.00001$, respectively). (**H**) In a new group of GFAP::hM4Di mice, CNO administration (n=12) only during the recall tests had no effect on either recent or remote memory, compared to Saline-injected controls (n=12). In these mice, CNO administration during recall also had no effect on auditory cued memory either 24 hr after acquisition (**I**) or 20 days after that (**J**), compared to Saline-injected controls. When CNO was not administered during acquisition of the non-associative place recognition task, the GFAP::hM4Di mice (n=6) from Figure 1L showed equivalent performance to controls (n=7; $p<0.01$)(**K**). Example exploration traces and average Δ are shown (*right*). Data presented as mean ± SEM.

Europe PMC Funders Author Manuscripts

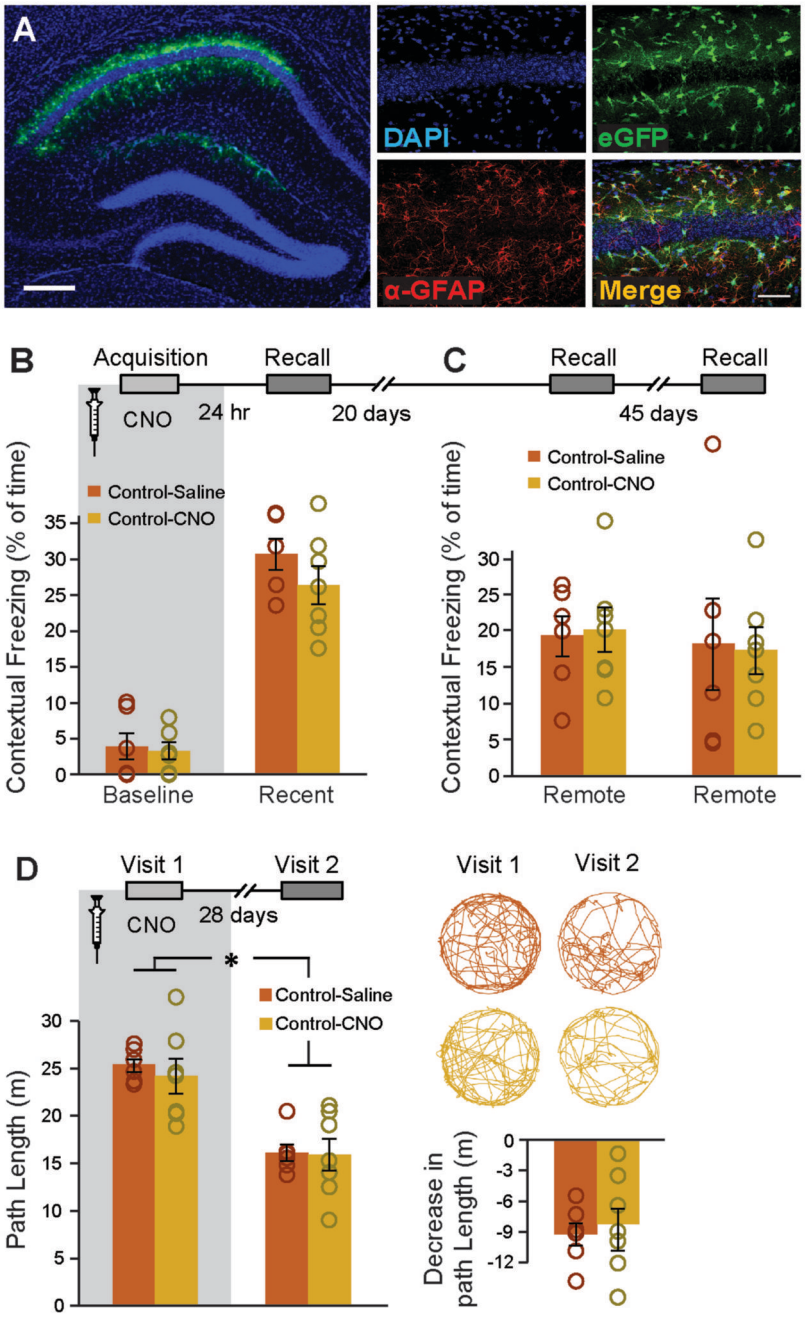

Extended Data Fig. 3. CNO application itself during learning had no effect on remote memory (Related to Figure 1).

(**A**) Bilateral double injection of AAV8-GFAP-eGFP resulted in eGFP expression in CA1 astrocytes only. Scale bar – left 300μm, right 50 μm. Mice expressing eGFP in their CA1 astrocytes were injected with either Saline (n=6) or CNO (n=7) 30min before fear conditioning acquisition. CNO administration before training to eGFP-expressing mice had no effect on baseline freezing or recent contextual memory recall one day later (**B**). Neither did CNO have any effect on remote memory 20 days later or 45 days after that (**C**). In

the non-associative place recognition test, CNO application before a first visit to a new environment had no effect on remote memory 28 days later (**D**), reflected by a similar decrease ($p<0.0001$) in the exploration between Saline injected (n=6) and CNO-treated mice (n=7) Example exploration traces and the average change (Δ) following treatment are shown on the right. Data presented as mean ± SEM.

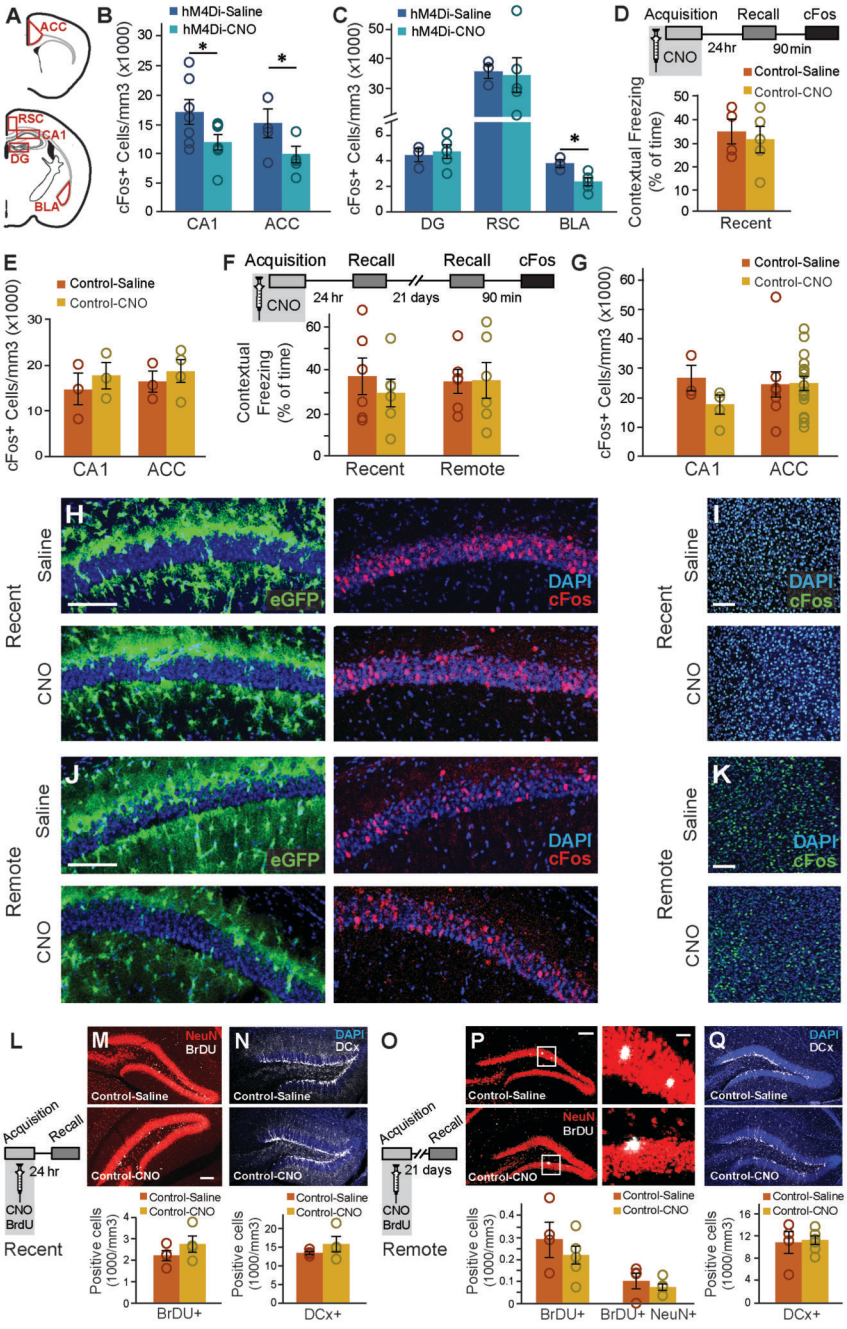

Extended Data Fig. 4. CNO administration during acquisition reduces CA1 and ACC activity at the time of remote recall only in GFAP::hM4Di mice, and does not affect neuronal proliferation, differentiation, or survival (Related to Figure 2).

Europe PMC Funders Author Manuscripts

(**A**) Active neurons expressing cFos were quantified in the CA1, ACC, dentate gyrus (DG), retrosplenial cortex (RSC), and basolateral amygdala (BLA). GFAP::hM4Di mice from figure 2A,B that were injected with CNO (n=6) before fear conditioning and showed impaired remote recall compared to Saline controls (n=6), also demonstrated reduced number of cFos expressing neurons in CA1 and ACC ($p<0.05$ for both)(**B**). No changes in cFos expression in the DG or RSC were observed in these mice, but the reduced fear was accompanied by a significant reduction in cFos expression in the BLA ($p<0.05$)(**C**). GFAP::eGFP control mice were injected with CNO (n=5) or Saline (n=5) before fear conditioning, and then tested on the next day. No changes were observed in recent memory (**D**) or in the number of neurons active during recent recall in the CA1 or ACC (**E**). Other GFAP::eGFP mice were injected with CNO (n=5) or Saline (n=6) before fear conditioning, and then tested on the next day and again 21 days later. No changes were observed in recent or remote memory (**F**), or in the number of neurons active during remote recall in the CA1 or ACC (**G**). Representative images of GFAP::eGFP (green) and cFos (red in H,J green in I,K) following recent (**H-I**) or remote (**J-K**) recall in the CA1 (**H,J**) and ACC (**I,K**) are presented. (**L**) GFAP::eGFP mice were injected with CNO or Saline together with BrdU before fear conditioning, and then tested on the next day. No changes were observed in stem cell proliferation (Brdu in white)(**M**) or in the number of young, Doublecortine (DCx)-positive neurons (white)(**N**). (**O**) GFAP::eGFP mice were injected with CNO or Saline and BrdU before fear conditioning, and then tested 21 days later. No changes were observed in stem cell proliferation and differentiation (**P**) or in the number of young, DCx-positive neurons (**Q**). Scale bars = 100μm for CA1, ACC and whole DG, 10 μm for zoomed-in cells. Data presented as mean ± SEM.

Europe PMC Funders Author Manuscripts

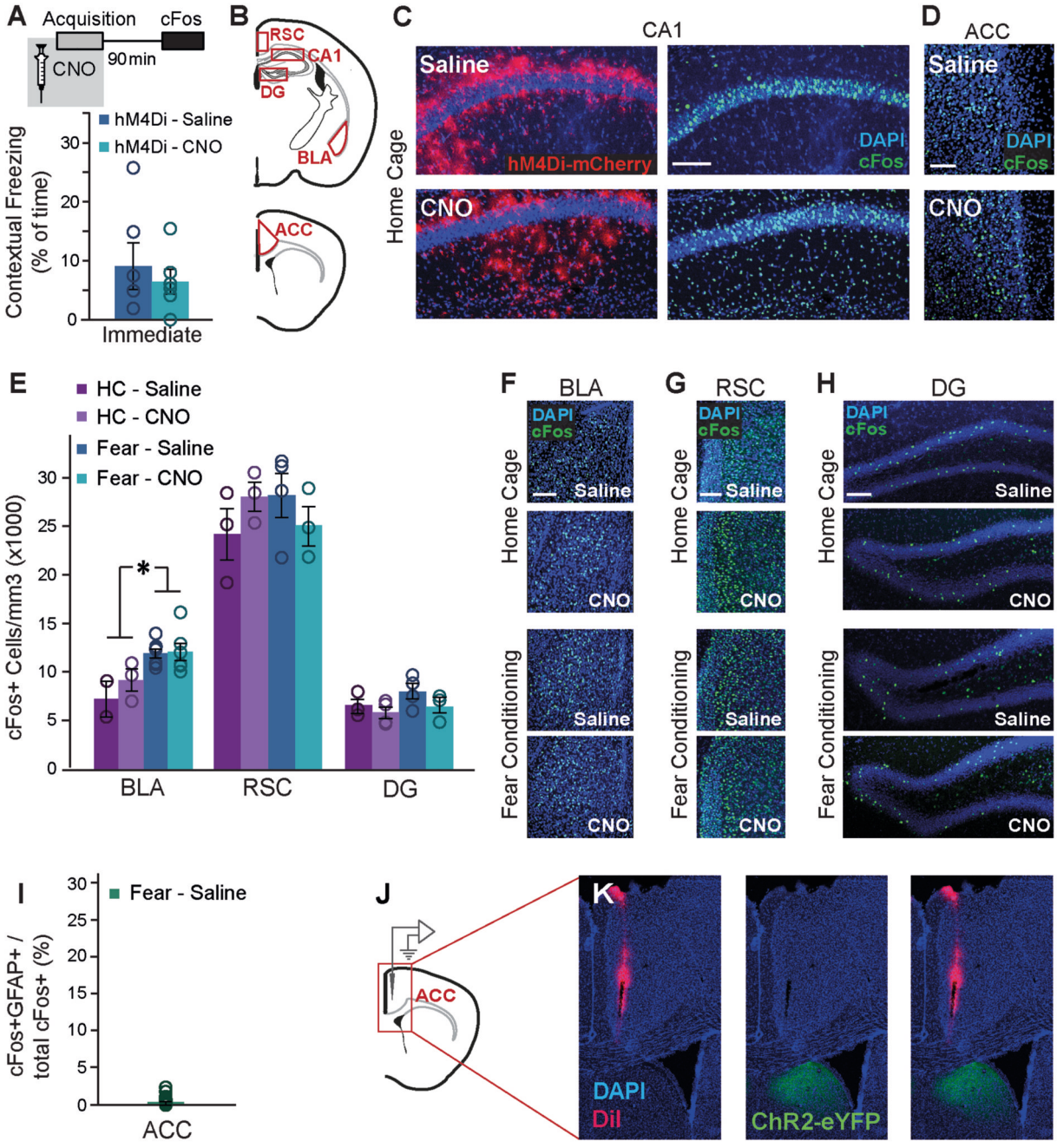

Extended Data Fig. 5. Gi pathway activation in CA1 astrocytes during memory acquisition does not affect the recruitment of the RSC and DG (Related to Figure 3).

(**A**) GFAP::hM4Di mice that were injected with CNO (n=9) or Saline (n=9) 30 minutes before fear conditioning showed similar immediate freezing following shock administration to Saline-injected controls. (**B**) Active neurons expressing cFos were quantified in the in the CA1, basolateral amygdala (BLA), ACC, retrosplenial cortex (RSC) and dentate gyrus (DG) of GFAP::hM4Di mice that were injected with CNO (n=9) or Saline (n=9) 30 minutes before fear conditioning, or in home-caged mice (CNO n=4, Saline n=4). (**C**)

Representative images of hM4Di (red) and cFos (green) in the CA1 (**C**) and ACC (**D**) of home caged GFAP::hM4Di mice showing no effect of CNO administration on cFos levels. cFos-expressing astrocytes are observed below and above the CA1 pyramidal layer. Scale bars=100μm. (**E**) Fear-conditioned GFAP::hM4Di mice showed increased cFos levels in the BLA compared to home-caged mice ($p<0.01$), but CNO administration had no effect on either group. Fear-conditioning and CNO administration had no effect on cFos levels in the RSC and DG. Representative images of hM4Di (red) and cFos (green) in the BLA (**F**), RSC (**G**) and DG (**H**) are presented. (**I**) Double staining for cFos and GFAP showed a negligible (0.34%) percent of ACC astrocytes that express cFos. (**J**) An electrode dipped in DiI was placed in the ACC to record the response to CA1 activation. (**K**) The location of the electrode in the ACC is shown in crimson, and no ChR2-eYFP positive axons (green) are observed in this region. All scale bars = 100μm. Data presented as mean ± SEM.

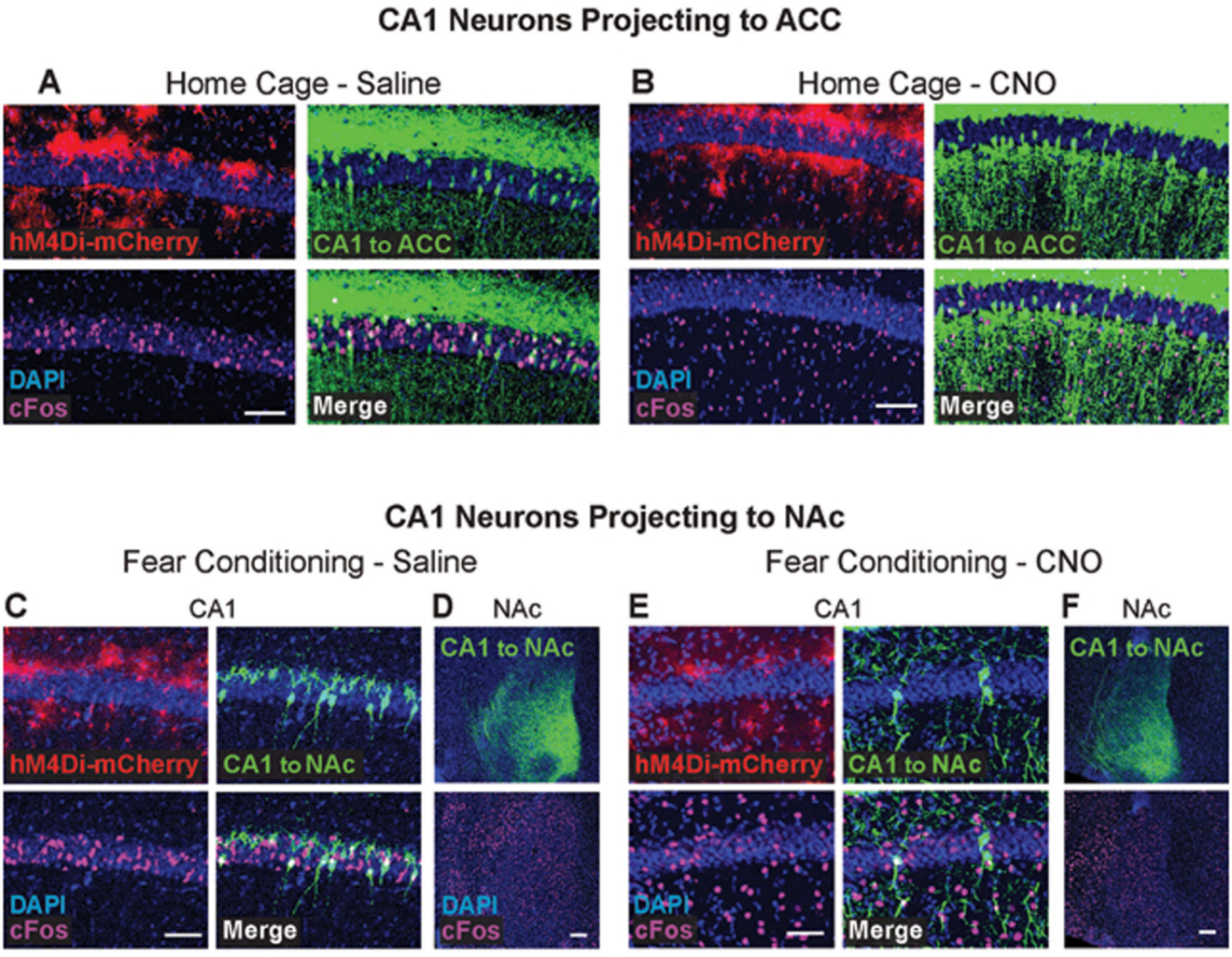

Extended Data Fig. 6. Gi pathway activation in CA1 astrocytes has no effect on cFos expression in home-caged mice (Related to Figure 4).

(**A-B**) Representative images of hM4Di in astrocytes (red), GFP in ACC-projecting CA1 neurons (green) and cFos (pink) in the CA1 of Saline- (**A**) or CNO- (**B**) injected home-caged

mice are presented. No effect of CNO on cFos levels was observed. (**C, E**) Representative images of hM4Di in astrocytes (red), GFP in NAc-projecting CA1 neurons (green) and cFos (pink) in the CA1 of Saline- (**C**) or CNO- (**E**) injected fear-conditioned mice are presented, showing no effect of the astrocytic manipulation on CA1→NAc neurons activity. The GFP-positive axons of these CA1 neurons are clearly observed in the NAc (**D,F**), with no apparent effect on cFos expression in this region. All scale bars=50μm.

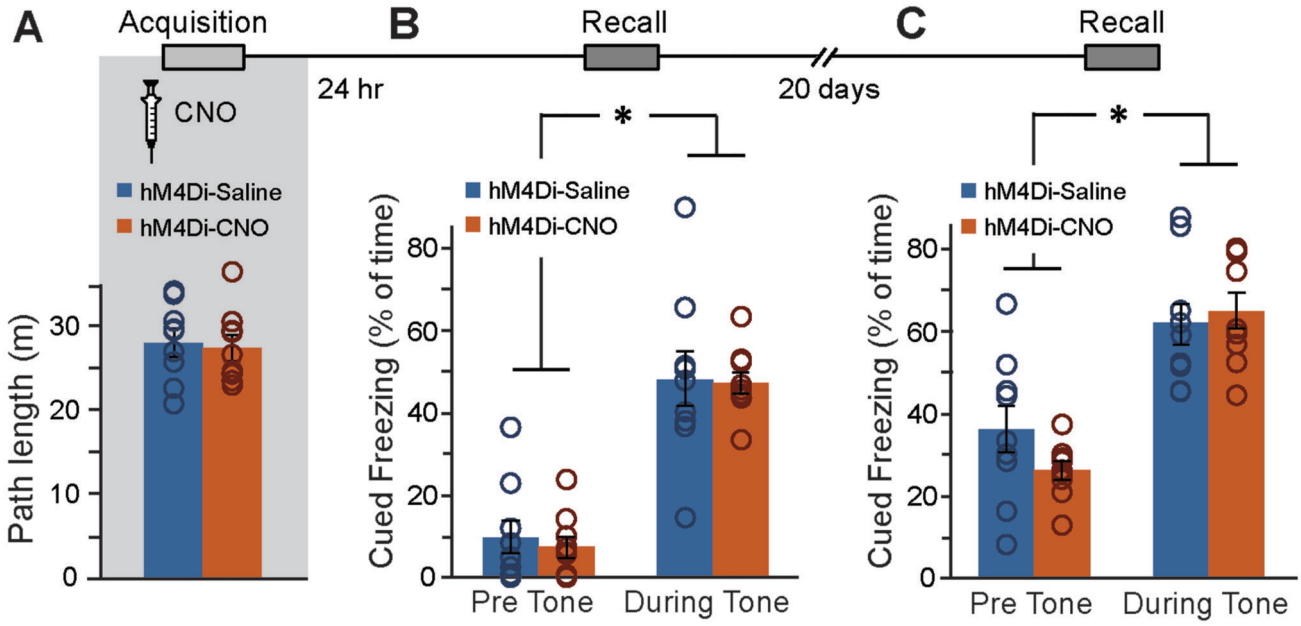

Extended Data Fig. 7. Specific inhibition of CA1-to-ACC projection during learning had no effect on auditory-cued memory (Related to Figure 5).

CA1→ACC-hM4Di mice were injected with Saline (n=9) or CNO (n=9) 30 min before FC acquisition. CNO application before training had no effect on exploration of the conditioning cage (**A**), or on auditory-cued memory recall either 24 hr after acquisition (**B**) or 20 days after that (**C**) in a novel context, with both groups showing increased freezing during tone presentation ($p<0.00001$, $p<0.0001$, respectively). Data presented as mean ± SEM.

Supplementary Material

Refer to Web version on PubMed Central for supplementary material.

Acknowledgments

We thank the entire Goshen lab for their support. AK is supported by the JBC GOLD Scholarship. AA is supported by the Adams fellowship. This project has received funding from the European Research Council (ERC) under the European Union's Horizon 2020 research and innovation programme (grant agreement No 803589 to IG). IG is also supported by the Israel Science Foundation (ISF grant No. 1815/18), the Israeli Centers of Research Excellence Program (center No. 1916/12), and the Canada-Israel grants (CIHR-ISF, grant No. 2591/18). ML is a Sachs Family Lecturer in Brain Science and is supported by the ISF (ISF grant No. 1024/17) and the Einstein Foundation. We thank Yaniv Ziv, Ami Citri, Inna Slutsky, and Adi Doron for the critical reading of the manuscript.

Data Availability

The data used to support the conclusions of this study is publicly available at: https://data.mendeley.com/datasets/5jw3dxhb87/1, as indicated in the Life Sciences Reporting Summary.

Code Availability

Analysis codes will be made available to any interested reader.

References

1. Moscovitch M, Cabeza R, Winocur G, Nadel L. Episodic Memory and Beyond: The Hippocampus and Neocortex in Transformation. Annual review of psychology. 2016; 67 :105–134.
2. Frankland PW, Bontempi B. The organization of recent and remote memories. Nature reviews Neuroscience. 2005; 6 :119–130. [PubMed: 15685217]
3. Doron A, Goshen I. Investigating the transition from recent to remote memory using advanced tools. Brain research bulletin. 2018; 141 :35–43. [PubMed: 28939475]
4. Araque A, et al. Gliotransmitters travel in time and space. Neuron. 2014; 81 :728–739. [PubMed: 24559669]
5. Durkee CA, Araque A. Diversity and Specificity of Astrocyte-neuron Communication. Neuroscience. 2019; 396 :73–78. [PubMed: 30458223]
6. Martin R, Bajo-Graneras R, Moratalla R, Perea G, Araque A. Circuit-specific signaling in astrocyte-neuron networks in basal ganglia pathways. Science. 2015; 349 :730–734. [PubMed: 26273054]
7. Perea G, Yang A, Boyden ES, Sur M. Optogenetic astrocyte activation modulates response selectivity of visual cortex neurons in vivo. Nature communications. 2014; 5 :3262.
8. Tan Z, et al. Glia-derived ATP inversely regulates excitability of pyramidal and CCK-positive neurons. Nature communications. 2017; 8 :13772.
9. Matos M, et al. Astrocytes detect and upregulate transmission at inhibitory synapses of somatostatin interneurons onto pyramidal cells. Nature communications. 2018; 9 :4254.
10. Deemyad T, Luthi J, Spruston N. Astrocytes integrate and drive action potential firing in inhibitory subnetworks. Nature communications. 2018; 9 :4336.
11. Savtchouk I, et al. Circuit-specific control of the medial entorhinal inputs to the dentate gyrus by atypical presynaptic NMDARs activated by astrocytes. Proceedings of the National Academy of Sciences of the United States of America. 2019; 116 :13602–13610. [PubMed: 31152131]
12. Martin-Fernandez M, et al. Synapse-specific astrocyte gating of amygdala-related behavior. Nature neuroscience. 2017; 20 :1540–1548. [PubMed: 28945222]
13. Adamsky A, et al. Astrocytic Activation Generates De Novo Neuronal Potentiation and Memory Enhancement. Cell. 2018; 174 :59–71. e14 [PubMed: 29804835]
14. Nagai J, et al. Hyperactivity with Disrupted Attention by Activation of an Astrocyte Synaptogenic Cue. Cell. 2019; 177 :1280–1292. e1220 [PubMed: 31031006]
15. Mederos S, et al. Melanopsin for precise optogenetic activation of astrocyte-neuron networks. Glia. 2019
16. Goshen I. The optogenetic revolution in memory research. Trends in neurosciences. 2014; 37 :511–522. [PubMed: 25022518]
17. Adamsky A, Goshen I. Astrocytes in Memory Function: Pioneering Findings and Future Directions. Neuroscience. 2018; 370 :14–26. [PubMed: 28571720]
18. Orr AG, et al. Astrocytic adenosine receptor A2A and Gs-coupled signaling regulate memory. Nature neuroscience. 2015; 18 :423–434. [PubMed: 25622143]
19. Durkee CA, et al. Gi/o protein-coupled receptors inhibit neurons but activate astrocytes and stimulate gliotransmission. Glia. 2019; 67 :1076–1093. [PubMed: 30801845]

Europe PMC Funders Author Manuscripts

20. Chai H, et al. Neural Circuit-Specialized Astrocytes: Transcriptomic, Proteomic, Morphological, and Functional Evidence. Neuron. 2017; 95 :531–549. e539 [PubMed: 28712653]
21. Santello M, Toni N, Volterra A. Astrocyte function from information processing to cognition and cognitive impairment. Nature neuroscience. 2019; 22 :154–166. [PubMed: 30664773]
22. Frankland PW, Bontempi B, Talton LE, Kaczmarek L, Silva AJ. The involvement of the anterior cingulate cortex in remote contextual fear memory. Science. 2004; 304 :881–883. [PubMed: 15131309]
23. Goshen I, et al. Dynamics of retrieval strategies for remote memories. Cell. 2011; 147 :678–689. [PubMed: 22019004]
24. Einarsson EO, Pors J, Nader K. Systems reconsolidation reveals a selective role for the anterior cingulate cortex in generalized contextual fear memory expression. Neuropsychopharmacology : official publication of the American College of Neuropsychopharmacology. 2015; 40 :480–487. [PubMed: 25091528]
25. Wheeler AL, et al. Identification of a functional connectome for long-term fear memory in mice. PLoS computational biology. 2013; 9 e1002853 [PubMed: 23300432]
26. Tayler KK, Tanaka KZ, Reijmers LG, Wiltgen BJ. Reactivation of neural ensembles during the retrieval of recent and remote memory. Current biology : CB. 2013; 23 :99–106. [PubMed: 23246402]
27. Makino Y, Polygalov D, Bolanos F, Benucci A, McHugh TJ. Physiological Signature of Memory Age in the Prefrontal-Hippocampal Circuit. Cell reports. 2019; 29 :3835–3846. e3835 [PubMed: 31851917]
28. Doron A, Goshen I. Investigating the transition from recent to remote memory using advanced tools. Brain research bulletin. 2017
29. Frankland PW, Josselyn SA. Hippocampal Neurogenesis and Memory Clearance. Neuropsychopharmacology : official publication of the American College of Neuropsychopharmacology. 2016; 41 :382–383. [PubMed: 26657960]
30. Kreisel T, Wolf B, Keshet E, Licht T. Unique role for dentate gyrus microglia in neuroblast survival and in VEGF-induced activation. Glia. 2019; 67 :594–618. [PubMed: 30453385]
31. Rajasethupathy P, et al. Projections from neocortex mediate top-down control of memory retrieval. Nature. 2015; 526 :653–659. [PubMed: 26436451]
32. Wang DV, Ikemoto S. Coordinated Interaction between Hippocampal Sharp-Wave Ripples and Anterior Cingulate Unit Activity. The Journal of neuroscience : the official journal of the Society for Neuroscience. 2016; 36 :10663–10672. [PubMed: 27733616]
33. Yu X, Nagai J, Khakh BS. Improved tools to study astrocytes. Nature reviews Neuroscience. 2020
34. Wang Y, et al. Accurate quantification of astrocyte and neurotransmitter fluorescence dynamics for single-cell and population-level physiology. Nature neuroscience. 2019; 22 :1936–1944. [PubMed: 31570865]
35. Martin-Fernandez M, et al. Synapse-specific astrocyte gating of amygdala-related behavior. Nature neuroscience. 2017
36. Barry DN, Coogan AN, Commins S. The time course of systems consolidation of spatial memory from recent to remote retention: A comparison of the Immediate Early Genes Zif268, c-Fos and Arc. Neurobiology of learning and memory. 2016; 128 :46–55. [PubMed: 26748021]
37. Lux V, Atucha E, Kitsukawa T, Sauvage MM. Imaging a memory trace over half a life-time in the medial temporal lobe reveals a time-limited role of CA3 neurons in retrieval. eLife. 2016; 5 e11862 [PubMed: 26880561]
38. Vetere G, et al. Chemogenetic Interrogation of a Brain-wide Fear Memory Network in Mice. Neuron. 2017; 94 :363–374. e364 [PubMed: 28426969]
39. Kitamura T, et al. Engrams and circuits crucial for systems consolidation of a memory. Science. 2017; 356 :73–78. [PubMed: 28386011]
40. DeNardo LA, et al. Temporal evolution of cortical ensembles promoting remote memory retrieval. Nature neuroscience. 2019; 22 :460–469. [PubMed: 30692687]
41. Teixeira CM, Pomedli SR, Maei HR, Kee N, Frankland PW. Involvement of the anterior cingulate cortex in the expression of remote spatial memory. The Journal of neuroscience : the official journal of the Society for Neuroscience. 2006; 26 :7555–7564. [PubMed: 16855083]

42. Ding HK, Teixeira CM, Frankland PW. Inactivation of the anterior cingulate cortex blocks expression of remote, but not recent, conditioned taste aversion memory. Learn Mem. 2008; 15 :290–293. [PubMed: 18441286]

Europe PMC Funders Author Manuscripts

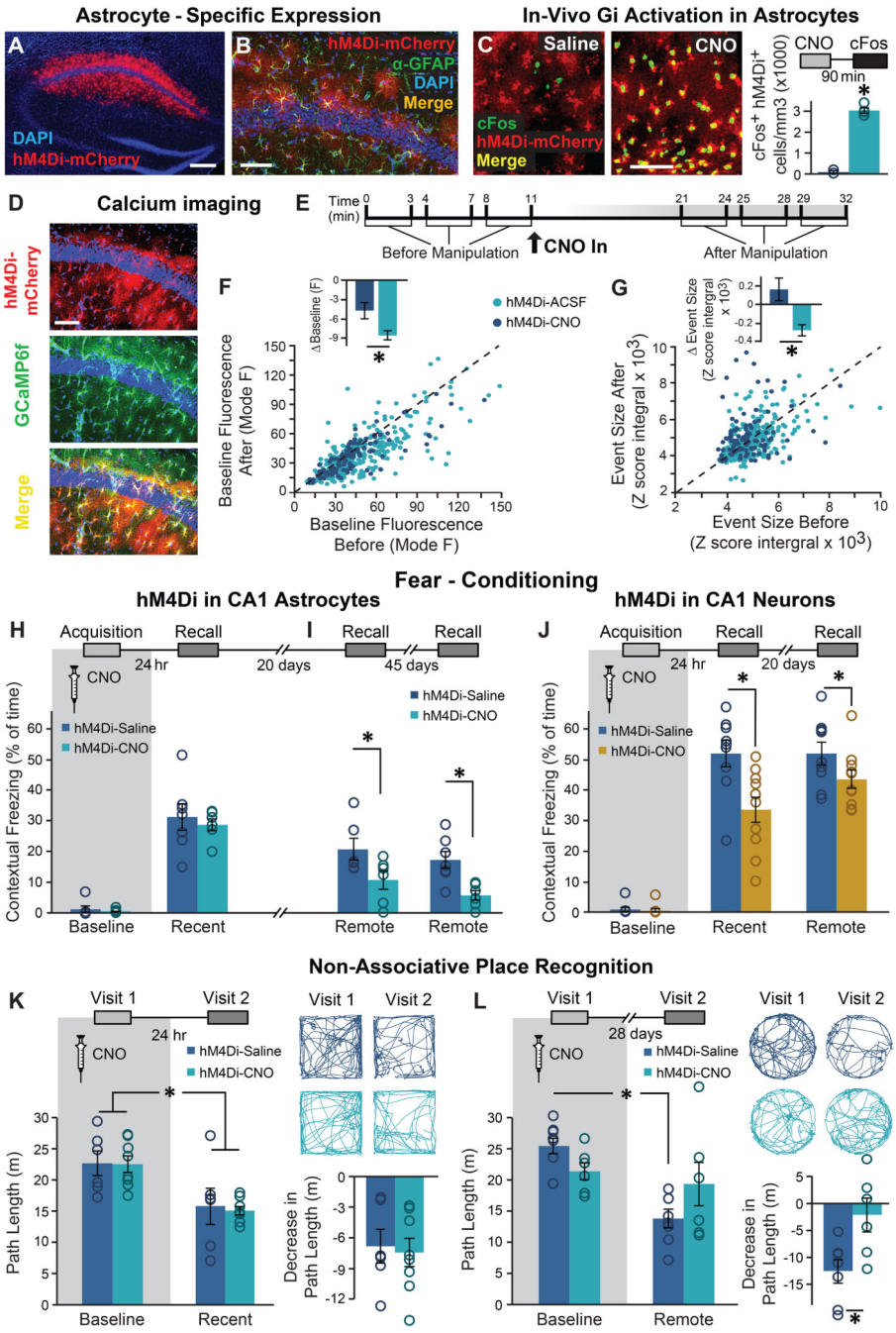

Figure 1. Astrocytic Gi pathway activation in CA1 during learning specifically impaired remote contextual memory.

(**A**) Bilateral double injection of AAV8-GFAP::hM4Di-mCherry resulted in hM4Di expression selectively in CA1 (scale bar 200μm). (**B**) hM4Di (red) was expressed in the astrocytic membrane around the soma, as well as in the distal processes (scale bar 50μm). (**C**) CNO administration in-vivo to mice expressing hM4Di (red) in CA1 astrocytes resulted in a significant increase in cFos expression (green) in these astrocytes, compared to Saline injected controls ($p<0.00005$, n = 2-4 mice, 6-15 slices per groups; scale bar 50μm). (**D**)

Europe PMC Funders Author Manuscripts

hM4Di-mCherry and GCaMP6f were co-expressed in CA1 astrocytes. (**E**) Astrocytes were imaged for 3x3min before and after application of ACSF (109 ROIs from 5 mice) or CNO (10μM; 299 ROIs from 8 mice). CNO application triggered a decrease in baseline intracellular Ca^{2+} levels, reflected by the mode of fluorescence levels ($p<0.01$)(**F**) and reduced the total size of Ca^{2+} events in these cells ($p<0.005$)(**G**), compared to astrocytes treated with ACSF. All ROIs are presented as dots in a scatter plot, and the average change (Δ) following treatment is plotted in the insert. (**H**) Mice expressing hM4Di in their CA1 astrocytes were injected with either Saline (n=7) or CNO (n=6) 30min before fear conditioning (FC) acquisition. CNO application before training had no effect on baseline freezing before shock administration or on recent contextual freezing on the next day compared to Saline treated controls. (**I**) CNO application before training resulted in a >50% impairment ($p<0.05$) in contextual freezing in CNO-treated mice tested 20 days later, compared to Saline treated controls (*left*). An even bigger impairment of >68% ($p<0.005$) was observed 45 days later (*right*). (**J**) Mice expressing hM4Di in their CA1 neurons were injected with either Saline (n=9) or CNO (n=10) 30min before FC acquisition. CNO application before training had no effect on baseline freezing before shock administration, bur resulted in decreased recent contextual freezing on the next day ($p<0.005$), and decreased remote recall 20 days after that ($p<0.05$) compared to Saline treated controls. (**K**) In the non-associative place recognition test, astrocytic Gi pathway activation by CNO application before a first visit to a new environment had no effect on recent memory, reflected by a similar decrease ($p<0.0001$) in the exploration between Saline injected (n=6) and CNO-treated mice (n=8). Example exploration traces andthe average change (Δ) in exploration following treatment are shown on the right. (**L**) Astrocytic modulation impaired remote recognition of the environment on the second visit, reflected by a decrease in the exploration only in the Saline injected (n=7)($p<0.01$), but not CNO-treated (n=6) mice. Example exploration traces and average decrease Δ are shown on the right. Data presented as mean ± standard error of the mean (SEM).

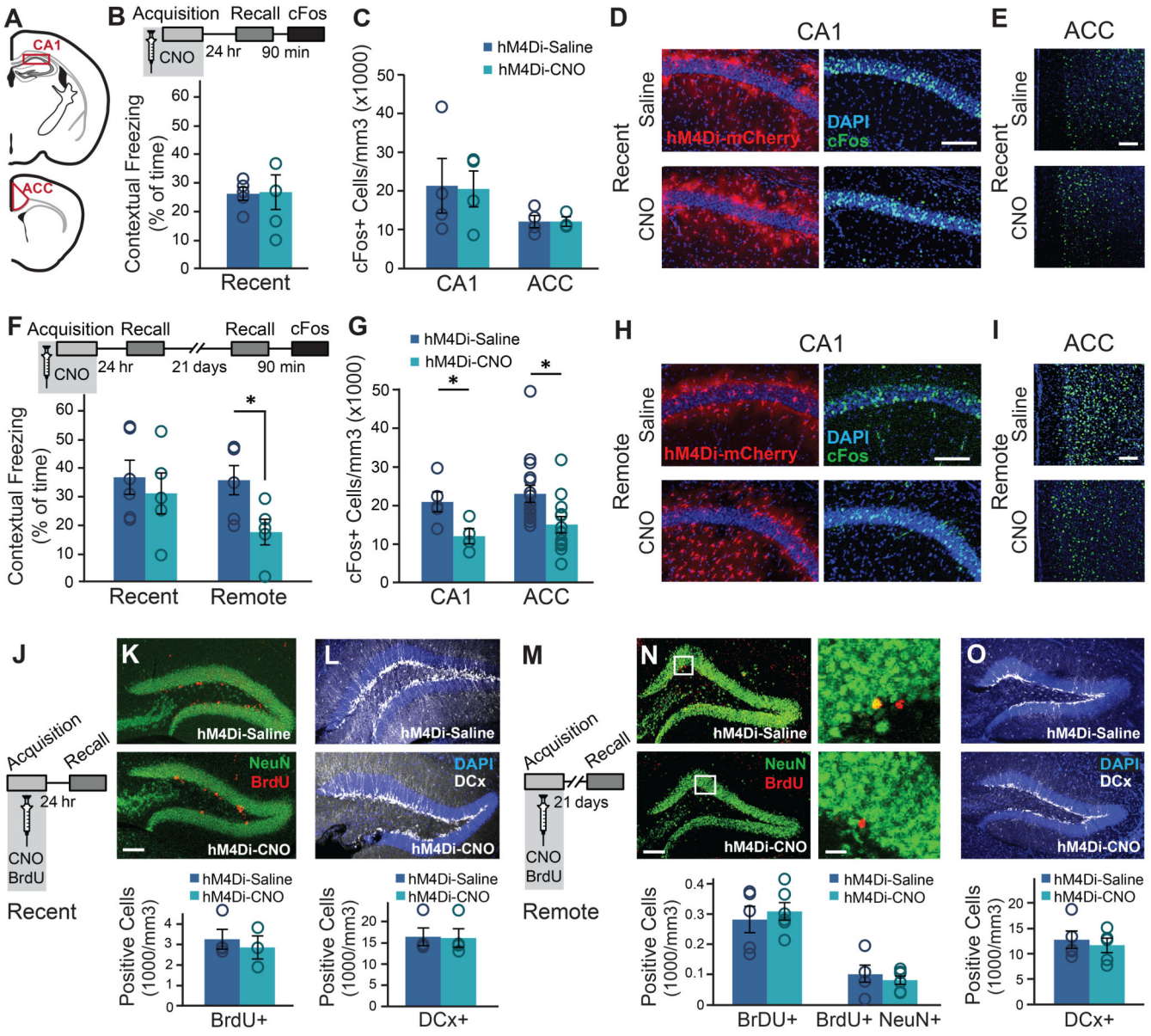

Figure 2. Astrocytic Gi activation during memory acquisition reduced CA1 and ACC activity at the time of remote recall, but did not affect neurogenesis

(**A**) Active neurons expressing cFos were quantified in the CA1 and ACC regions. GFAP::hM4Di mice were injected with CNO (n=5) or Saline (n=5) before fear conditioning, and then tested on the next day. No changes were observed in recent memory (**B**) or in the number of neurons active during recall in the CA1 or ACC (**C**). Representative images of hM4Di (red) and cFos (green) in the CA1 (**D**) and ACC (**E**) are presented. Other GFAP::hM4Di mice were injected with CNO (n=5) or Saline (n=6) before fear conditioning, and then tested on the next day and again 21 days later. No changes were observed in recent memory (**F** *left*). However, CNO application before training resulted in >50% reduction ($p<0.05$) in contextual freezing 21 days later, compared to Saline treated controls (**F** *right*). Impaired remote recall was accompanied by reduced number of cFos-expressing neurons

in CA1 and ACC ($p<0.05$ and $p<0.01$, respectively)(**G**). Representative images of the CA1 (**H**) and ACC (**I**) are presented. (**J**) GFAP::hM4Di mice were injected with CNO (n=5) or Saline (n=5) together with BrdU before fear conditioning, and then tested on the next day. No changes were observed in stem cell proliferation (Brdu in red)(**K**) or in the number of young, Doublecortine (DCx)-positive neurons (white)(**L**). (**M**) GFAP::hM4Di mice were injected with CNO (n=5) or Saline (n=6) and BrdU before fear conditioning, and then tested 21 days later. No changes were observed in stem cell proliferation and differentiation (**N**) or in the number of young, DCx-positive neurons (**O**). All scale bars = 100μm, except zoomed-in image in panel N where scale bar = 10μm. Data presented as mean ± SEM.

Europe PMC Funders Author Manuscripts

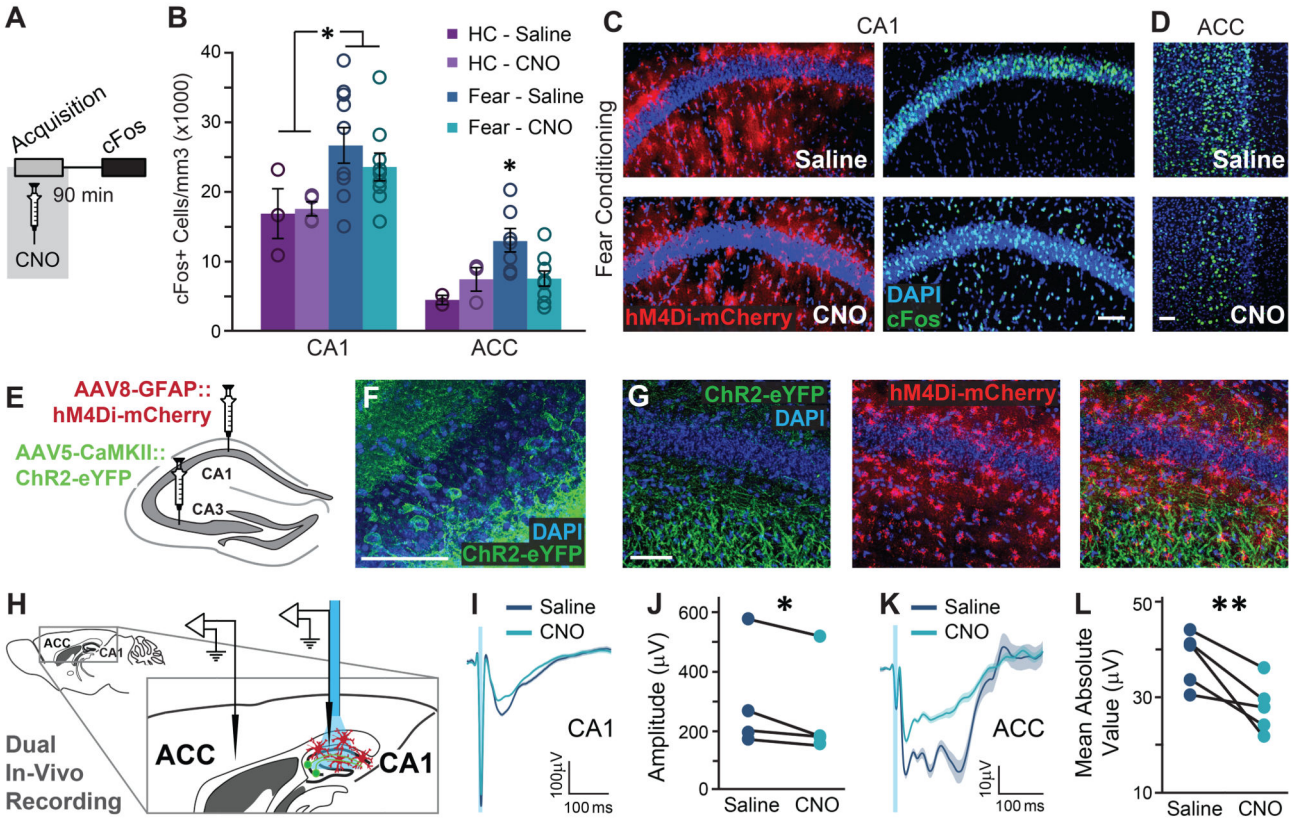

Figure 3. Astrocytic Gi activation in the CA1 prevents the recruitment of the ACC during memory acquisition, and inhibits CA1 to ACC communication.

(**A**) GFAP::hM4Di mice were injected with CNO (n=9) or Saline (n=9) 30 minutes before fear conditioning, and brains were removed 90 minutes later for cFos quantification. (**B**) Fear-conditioned GFAP::hM4Di mice showed increased cFos levels in the CA1 compared to home-caged mice ($p<0.01$), but CNO administration had no effect on either group. cFos levels in the ACC were increased in GFAP::hM4Di that underwent conditioning after being injected with Saline ($p<0.05$), but not in CNO-injected mice. Data presented as mean ± SEM. Representative images of hM4Di (red) and cFos (green) in the CA1 (**C**) and ACC (**D**) of fear-conditioned mice are presented. cFos-expressing astrocytes are observed below and above the CA1 pyramidal layer in CNO-treated mice. (**E**) AAV5-CaMKII::Channelrhodopsin-2(ChR2)-eYFP was injected into the CA3 and AAV8-GFAP::hM4Di-mCherry into CA1. (**F**) ChR2-eYFP was expressed in the soma of CA3 pyramidal cells. (**G**) The ChR2-expressing axons (green) are observed in the CA1 *stratum radiatum*, and hM4Di-expressing astrocytes (red) are observed in CA1. (**H**) Experimental setup: Light was applied to CA1 in anesthetized mice. The response to Schaffer collaterals optogenetic stimulation was simultaneously recorded in the CA1 and ACC, after Saline administration, followed by CNO administration. (**I-J**) The response in the CA1 to Schaffer collaterals optogenetic stimulation had a smaller amplitude under Gi-pathway activation by CNO in CA1 astrocytes (n= 4 mice; $p<0.05$). The average responses (**I**) from one mouse under Saline and then under CNO are presented (average in a bold line, SEM in shadow,

Europe PMC Funders Author Manuscripts

blue light illumination in semi-transparent blue). (**K-L**) A downstream response of CA1 activation by Schaffer collaterals optogenetic stimulation was detected in the ACC. The mean absolute value of the complex ACC response was found to have significantly smaller amplitude under Gi-pathway activation by CNO in CA1 astrocytes (n= 5 mice; $p<0.01$). The average responses (**K**) from one mouse under Saline and then under CNO are presented (average in a bold line, SEM in shadow). All scale bars=50μm.

Europe PMC Funders Author Manuscripts

Europe PMC Funders Author Manuscripts

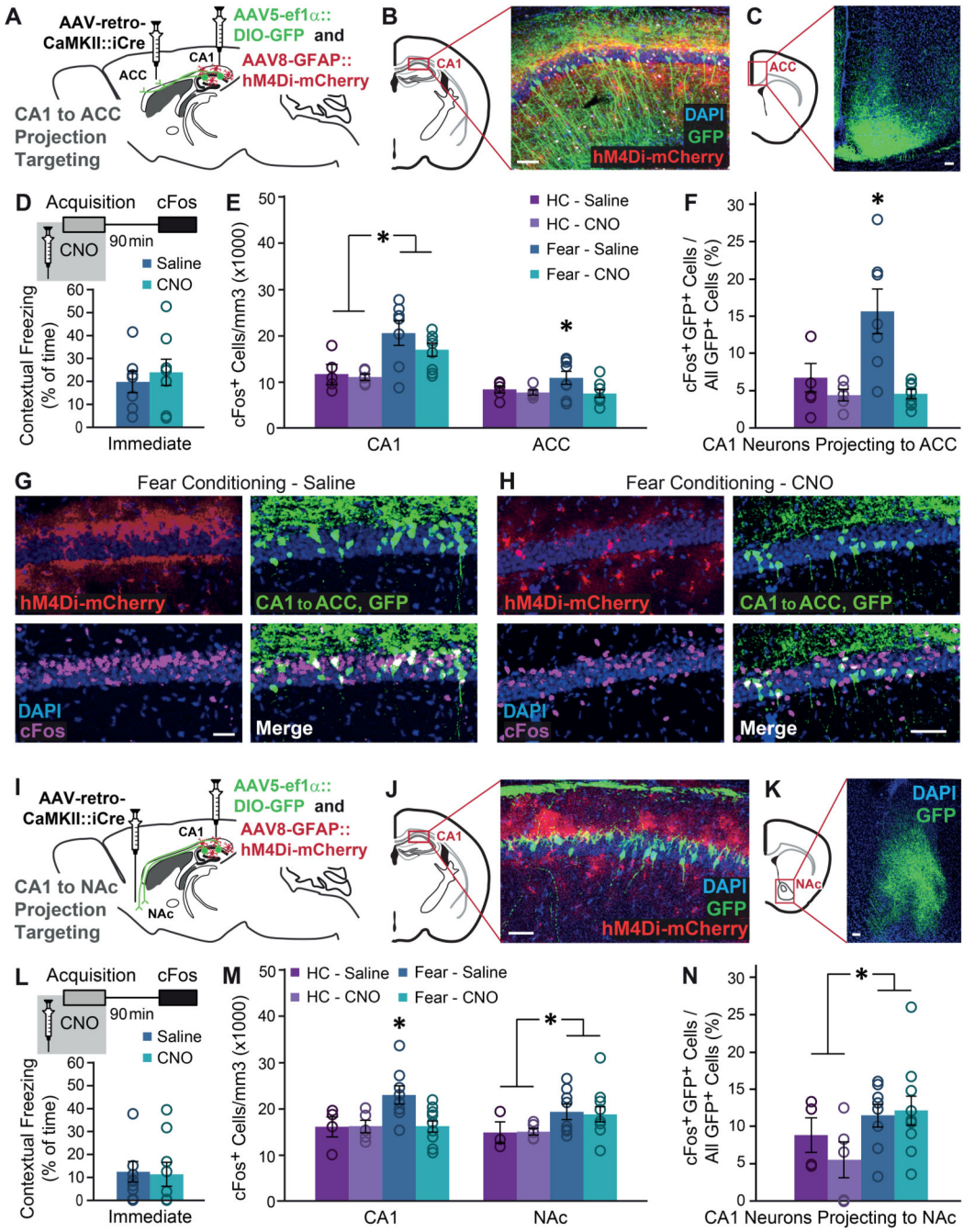

Figure 4. Gi pathway activation in CA1 astrocytes during memory acquisition specifically prevents the recruitment of CA1 neurons projecting to ACC.

(**A**) AAV-retro-CaMKII::Cre was injected into the ACC, and AAV5-ef1α::DIO-GFP together with AAV8-GFAP::hM4Di-mCherry were injected into CA1. (**B**) Together, these three vectors induced the expression of GFP (green) in CA1 neurons projecting to the ACC, and hM4Di (red) in CA1 astrocytes. (**C**) GFP-positive axons of CA1 projection neurons are clearly visible in the ACC. (**D**) Mice expressing GFP in ACC-projecting CA1 neurons and hM4Di in their CA1 astrocytes that were injected with CNO (n=8) or Saline (n=7)

30 minutes before FC showed similar immediate freezing following shock administration. (**E**) Fear-conditioned mice showed increased cFos levels in the CA1 compared to home-caged mice ($p<0.05$), with no effect for CNO administration. cFos levels in the ACC were increased in mice that underwent conditioning after being injected with Saline ($p<0.05$), but not in CNO-injected mice. (**F**) Fear-conditioned mice injected with Saline showed an >130% increase in the percent of CA1 cells projecting into the ACC that express cFos, compared to home-caged mice ($p<0.05$). CNO administration completely abolished the recruitment of these cells during learning. Representative images of hM4Di in astrocytes (red), GFP in ACC-projecting CA1 neurons (green) and cFos (pink) in the CA1 of Saline- (**G**) or CNO- (**H**) injected mice are presented. (**I**) AAV-retro-CaMKII::Cre was injected into the NAc, and AAV5-ef1α::DIO-GFP together with AAV8-GFAP::hM4Di-mCherry were injected into CA1. (**J**) Together, these three vectors induced the expression of GFP (green) in CA1 neurons projecting to the NAc, and hM4Di (red) in CA1 astrocytes. (**K**) GFP-positive axons of CA1 projection neurons are clearly visible in the NAc. (**L**) Mice expressing GFP in NAc-projecting CA1 neurons and hM4Di in their CA1 astrocytes that were injected with CNO (n=10) or Saline (n=8) 30 minutes before FC showed similar immediate freezing following shock administration. (**M**) Fear-conditioned mice showed increased cFos levels in the NAc compared to home-caged mice ($p<0.05$), with no effect for CNO administration. (**N**) Fear-conditioned mice injected with either Saline or CNO showed an >60% increase in the percent of CA1 cells projecting into the NAc that express cFos, compared to home-caged mice ($p<0.05$). CNO administration had no effect on the recruitment of these cells during learning. All scale bars=50μm. Data presented as mean ± SEM.

Europe PMC Funders Author Manuscripts

Europe PMC Funders Author Manuscripts

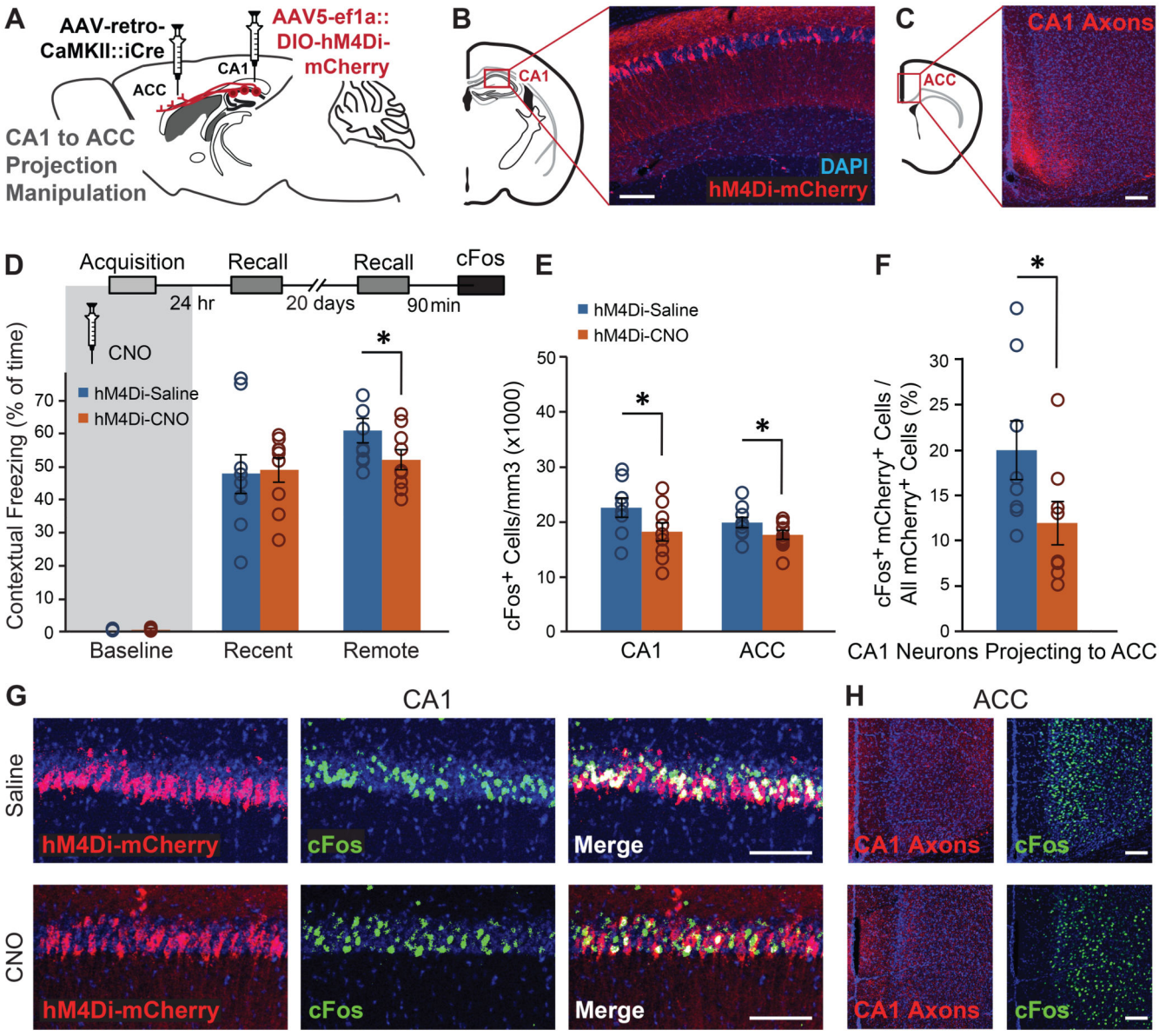

Figure 5. Specific inhibition of CA1-to-ACC projection during learning impairs the acquisition of remote, but not recent, memory.

(**A**) AAV-retro-CaMKII::Cre was injected into the ACC, and AAV5-ef1α::DIO-hM4Di-mCherry was injected into CA1. (**B**) Together, these vectors induced the expression of hM4Di-mCherry (red) in CA1 neurons projecting to the ACC. (**C**) hM4Di-mCherry-positive axons of CA1 projection neurons are clearly visible in the ACC. (**D**) Mice expressing hM4Di in their ACC-projecting CA1 neurons were injected with either Saline (n=9) or CNO (n=9) 30min before FC acquisition. CNO application before training had no effect on baseline freezing (*left*) before shock administration or on recent contextual freezing (*middle*) on the next day, but induced a significant decrease ($p<0.05$) 20 days later, compared to Saline treated controls (*right*). (**E**) Active neurons expressing cFos were quantified in the CA1 and ACC regions. Impaired remote recall was accompanied by reduced number of

cFos-expressing neurons in CA1 and ACC ($p<0.05$ for both). (**F**) CNO administration reduced the recruitment of CA1→ACC cells during remote recall. Representative images of hM4Di (red) and cFos (green) in the CA1 (**G**) and ACC (**H**) are presented. All scale bars = 100μm. Data presented as mean ± SEM.

Europe PMC Funders Author Manuscripts